AGU PUBLICATIONS

JGR

Journal of Geophysical Research: Atmospheres

RESEARCH ARTICLE

10.1002/2013JD020925

Key Points:

- Meteorology controls sea salt reaching Antarctica on interannual timescales
- Glacial increase in sea ice could almost double sea salt reaching Antarctica
- Sea salt proxy shows decreasing sensitivity approaching glacial sea ice extent

Supporting Information:

- Readme
- Text S1
- Figure S1
- Figure S2
- Figure S4
- Figure S5
- Figure S6
- Figure S7
- Figure S8

Correspondence to:
J. G. Levine,
j.g.levine@bham.ac.uk

Citation:
Levine, J. G., X. Yang, A. E. Jones, and E. W. Wolff (2014), Sea salt as an ice core proxy for past sea ice extent: A process-based model study, *J. Geophys. Res. Atmos.*, *119*, 5737–5756, doi:10.1002/2013JD020925.

Received 24 SEP 2013
Accepted 5 APR 2014
Accepted article online 9 APR 2014
Published online 14 MAY 2014

Sea salt as an ice core proxy for past sea ice extent: A process-based model study

J. G. Levine[1,2], X. Yang[3,4,5], A. E. Jones[1], and E. W. Wolff[1,6]

[1]British Antarctic Survey, Cambridge, UK, [2]Now at School of Geography, Earth and Environmental Sciences, University of Birmingham, Birmingham, UK, [3]Centre for Atmospheric Science, Department of Chemistry, University of Cambridge, Cambridge, UK, [4]National Centre for Atmospheric Science—Climate, University of Cambridge, Cambridge, UK, [5]Now at British Antarctic Survey, Cambridge, UK, [6]Department of Earth Sciences, University of Cambridge, Cambridge, UK

Abstract Sea ice is a reflection of, and a feedback on, the Earth's climate. We explore here, using a global atmospheric chemistry-transport model, the use of sea salt in Antarctic ice cores to obtain continuous long-term, regionally integrated records of past sea ice extent, synchronous with ice core records of climate. The model includes the production, transport, and deposition of sea salt aerosol from the open ocean and "blowing snow" on sea ice. Under current climate conditions, we find that meteorology, not sea ice extent, is the dominant control on the atmospheric concentration of sea salt reaching coastal and continental Antarctic sites on interannual timescales. However, through a series of idealized sensitivity experiments, we demonstrate that sea salt has potential as a proxy for larger changes in sea ice extent (e.g., glacial-interglacial). Treating much of the sea ice under glacial conditions as a source of salty blowing snow, we demonstrate that the increase in sea ice extent alone (without changing the meteorology) could drive, for instance, a 68% increase in atmospheric sea salt concentration at the site of the Dome C ice core, which exhibits an approximate twofold glacial increase in sea salt flux. We also show how the sensitivity of this potential proxy decreases toward glacial sea ice extent—the basis of an explanation previously proposed for the lag observed between changes in sea salt flux and δD (an ice core proxy for air temperature) at glacial terminations. The data thereby permit simultaneous changes in sea ice extent and climate.

1. Introduction

Sea ice is both a reflection of, and a feedback on, the Earth's climate. It is also a source of chemically reactive trace gases that profoundly affect polar springtime tropospheric chemistry [e.g., *Jones et al.*, 2006, 2009, 2010; *Yang et al.*, 2005, 2008, 2010; *Saiz-Lopez et al.*, 2007; *Abbatt et al.*, 2012] and an interface that partly governs the exchange of heat and greenhouse gases between the ocean and atmosphere at high latitudes [e.g., *Stephens and Keeling*, 2000; *Brunke et al.*, 2006; *Kurtz et al.*, 2011; *Parmentier et al.*, 2013]. A continuous record of past sea ice extent and its coevolution with climate would therefore be valuable, and the aim of this study is to explore in a process-based fashion the potential of sea salt in Antarctic ice cores to contribute to one. The use of sea salt as a sea ice proxy was first proposed by *Wolff et al.* [2003], and the developments since have recently been reviewed by *Abram et al.* [2013] (alongside the use of methyl sulphonic acid as an alternative ice core proxy). Traditionally, diatom assemblages in marine sediment cores have been used to infer when transitions between permanent sea ice, seasonal sea ice, and permanent open ocean have taken place at specific sites [e.g., *Gersonde et al.*, 2005]; we also note the increasing interest in sea ice biomarkers, such as the highly branched isoprenoid (HBI) biomarker, IP_{25}, understood to be produced by diatoms as the sea ice retreats in local spring [*Belt et al.*, 2007; *Belt and Müller*, 2013]. It remains difficult, however, to piece together from these site-specific records a polar-wide picture of sea ice extent and, especially, the temporal evolution of that polar-wide picture. Figure 4 of *Gersonde et al.* [2005], for instance, indicates the areas of uncertainty that remain in the diatom-based reconstruction of Antarctic sea ice at the Last Glacial Maximum (LGM), despite a concerted marine-coring effort. Here, building on previous modeling efforts [e.g., *Genthon*, 1992; *Gong et al.*, 1997, 2002; *Reader and McFarlane*, 2003; *Mahowald et al.*, 2006], we use a global atmospheric chemistry-transport model to explore the potential of sea salt in Antarctic ice cores to provide continuous long-term, regionally integrated records of sea ice extent to complement the site-specific records. Antarctic ice cores have yielded records of climate and atmospheric composition spanning up to the last 800,000 years, or eight glacial-interglacial cycles [e.g., *Wolff et al.*, 2006; *Jouzel et al.*, 2007; *Loulergue et al.*, 2008; *Lüthi et al.*, 2008], and sea salt in ice cores could potentially provide synchronous records of sea ice extent of equal length.

Uncertainties remain regarding the mechanistic link between the supply of sea salt to Antarctic sites and sea ice extent. If the open ocean (i.e., the bursting of air bubbles at the surface created by wave breaking) were the dominant source of sea salt reaching these sites, we might expect to observe higher atmospheric sea salt concentrations there during periods of less extensive sea ice—local summer compared to local winter and interglacial periods compared to glacial ones—when the distance between the open ocean and those sites is shorter, and presumably less sea salt aerosol (SSA) is deposited en route. That is, provided the meteorology, governing the production of SSA, its transport to each site, and deposition en route, does not change. However, almost without exception, the atmospheric concentration of sea salt reaching Antarctic sites exhibits a maximum in local winter, for example, at Halley Bay and Neumayer [*Wagenbach et al.*, 1998], Kohnen Station [*Weller and Wagenbach*, 2007], and Concordia Station [*Jourdain et al.*, 2008; *Udisti et al.*, 2012]. The only exception is Dumont D'Urville, where a summer maximum is observed [*Wagenbach et al.*, 1998]. The flux of sea salt recorded in Antarctic ice also exhibits winter maxima but, paradoxically, does not show any clear, consistent dependence on sea ice extent, on interannual timescales at least; see review of *Abram et al.* [2013] and the references contained therein. *Abram et al.* [2013] conclude that sea salt in Antarctic ice cores appears to be an unpromising indicator of interannual changes in sea ice extent, with other factors, such as changes in atmospheric transport and/or the occurrence of polynyas [e.g., *Kaspari et al.*, 2005; *Criscitiello et al.*, 2013], exerting greater influence on sea salt flux on these timescales. However, Antarctic ice cores also reliably exhibit maxima in sea salt flux during past glacial periods, when sea ice was far more extensive than today, for example, at Vostok [*Petit et al.*, 1999], Dome C [*Wolff et al.*, 2006, 2010], Talos Dome [*Iizuka et al.*, 2013], and Dome Fuji [*Sato et al.*, 2013]. The flux of sea salt at the LGM, for example, was approximately 2–3 times that in the Holocene; see review of *Fischer et al.* [2007a] and the references therein. Perhaps sea salt remains a viable proxy on longer timescales, subject to larger changes in sea ice extent.

Increased storminess in local winter and glacial periods (cf. local summer and interglacial periods), if it occurred, could drive an increase in SSA production from the open ocean and/or faster meridional transport to Antarctic sites [see, e.g., *Petit et al.*, 1999; *Fischer et al.*, 2007a]. The colder, drier conditions during those periods could also yield somewhat longer SSA lifetimes with respect to wet deposition [see, e.g., *Petit and Delmonte*, 2009]. However, it has recently been proposed that an additional source of SSA directly associated with the sea ice could be responsible for the winter and glacial maxima in atmospheric sea salt concentration and ice core sea salt flux. This is on the assumption that the sea ice source constitutes a stronger source than the open ocean the sea ice replaces. Several such sources have been proposed, including frost flowers [e.g., *Rankin et al.*, 2002, 2004; *Kaleschke et al.*, 2004; *Roscoe et al.*, 2011], brine [e.g., *Perovich and Richter-Menge*, 1994; *Wagenbach et al.*, 1998; *Rankin et al.*, 2000], and "blowing snow" on sea ice [*Yang et al.*, 2008, 2010]. One or more of these sources, which have direct contact with the cold sea ice surface, could also explain observations of so-called "negative non-sea-salt sulphate" [e.g., *Wagenbach et al.*, 1998; *Rankin et al.*, 2000; *Rankin and Wolff*, 2003; *Jourdain et al.*, 2008]. This is essentially the deficit, relative to bulk seawater, in the ratio of sulphate to sodium ion concentrations, $[SO_4^{2-}(aq)]$:$[Na^+(aq)]$, frequently observed in SSA reaching coastal, and at least some central Antarctic sites, in local winter. We might expect the $[SO_4^{2-}(aq)]$:$[Na^+(aq)]$ ratio in SSA to match that of bulk seawater or to perhaps exceed it as a result of the addition of sulphate from non-sea-salt sources during transport, such as dust and the oxidation products of dimethyl sulphide and sulphur dioxide. However, there is a process that could account for the observations of "negative non-sea-salt sulphate": the precipitation of mirabilite ($Na_2SO_4 \cdot 10H_2O$), which reduces the $[SO_4^{2-}(aq)]$:$[Na^+(aq)]$ ratio of the sea salt source relative to bulk seawater by preferentially removing sulphate ions [e.g., *Wagenbach et al.*, 1998]. Crucially, this process only occurs at temperatures below $-8\,°C$—temperatures not encountered at the ocean surface but frequently encountered at the winter sea ice surface.

Of the sea ice sources proposed, "blowing snow" [*Yang et al.*, 2008, 2010] also shows skill at explaining a key feature of polar tropospheric chemistry: the springtime enhancement in the concentrations of reactive bromine-containing trace gases, such as bromine monoxide (BrO). These reactive gases, of which SSA is a major source, are responsible for springtime tropospheric ozone depletion events [e.g., *Jones et al.*, 2006, 2009, 2010; *Yang et al.*, 2005, 2008, 2010; *Saiz-Lopez et al.*, 2007; *Abbatt et al.*, 2012]. Importantly, *Yang et al.* [2010] explored the ability of a global atmospheric chemistry-transport model to reproduce observed enhancements in tropospheric column [BrO] (based on GOME satellite measurements) at Barrow in the Arctic spring of 1998. They found that a simulation employing only an open ocean source of SSA could not capture the observed enhancements, but one also employing their "blowing snow" source captured much of their scale and timing; see their Figure 3. *Yang et al.* [2008] propose that this blowing snow source operates as follows: snow falling on seasonal or sufficiently thin sea ice suppresses it, causing it to be flooded with salty sea water; the snow is thus made salty, and if lofted by strong winds, may sublime to yield SSA. Though at present a hypothetical, if plausible source, its feasibility is currently being critically examined through field measurements.

Previous model studies of changes in the supply of sea salt to Antarctica under glacial conditions either did not include a sea ice source of SSA [*Genthon*, 1992] or included only a relatively simple one, not specific to the sea ice environment [*Reader and McFarlane*, 2003; *Mahowald et al.*, 2006]. *Reader and McFarlane* [2003] explored the implications of (i) a constant flux of sea salt from all ice-covered ocean and (ii) an empirically determined flux constrained by the sea salt concentration measurements of *Erickson et al.* [1986]. *Mahowald et al.* [2006] instead extended their application of the open ocean source of *Monahan et al.* [1986] to regions of sea ice, exploring the consequences of treating (i) all sea ice and (ii) only newly formed sea ice as a source of sea salt. Here, we use the same global atmospheric chemistry-transport model that *Yang et al.* [2010] used, including their process-based blowing snow source of SSA—that can not only explain observations of so-called "negative non-sea-salt sulphate" but also shows skill at explaining the observed springtime enhancement in polar tropospheric [BrO]—as well as the open ocean source of *Monahan et al.* [1986]. While *Yang et al.* [2010] simulated the production of SSA, and the transport and chemistry of reactive bromine-containing trace gases derived from it (at source), we simulate the transport and deposition of the SSA itself. Specifically, we carry out a series of highly idealized sensitivity experiments designed to explore: whether, on interannual timescales, sea ice extent or meteorology principally controls the atmospheric concentration of sea salt sodium, referred to from here on simply as the concentration of sea salt, at Antarctic sites; what impact switching from recent to glacial sea ice extent has on the concentration of sea salt we simulate reaching these sites; and, if the concentration of sea salt changes with sea ice extent, how the sensitivity of this potential proxy varies as a function of sea ice extent. The model and sensitivity experiments are described in the next section, the results are presented in section 3, and we discuss their implications in section 4.

2. Sensitivity Experiments With the Cambridge p-TOMCAT Model

2.1. The Cambridge p-TOMCAT Model

The Cambridge parallelised-Tropospheric Offline Model of Chemistry and Transport (p-TOMCAT) is a 3-D global Eulerian model that has been used in a wide range of studies of atmospheric chemistry and transport [e.g., *Warwick et al.*, 2006, 2013; *Levine et al.*, 2007, 2011a, 2011b, 2012; *Yang et al.*, 2005, 2010]. It is driven by winds, temperatures, and humidities based on the operational analyses of the European Centre for Medium-Range Weather Forecasts (ECMWF) and utilizes monthly mean fields of fractional sea ice coverage based on the Hadley Centre Sea Ice and Sea Surface Temperature (HadISST) data set [*Rayner et al.*, 2003]. To explore the impact of switching from recent to glacial sea ice extent, we employ analogous fields based on sea surface temperatures (SSTs) from a gridded version of the Glacial Atlantic Ocean Mapping (GLAMAP) data set [*Sarnthein et al.*, 2003; *Paul and Schäfer Neth*, 2003a; *Paul and Schäfer-Neth*, 2003b]; we use the GLAMAP line version of *Paul and Schäfer-Neth* [2003b] based on the LGM SST isolines of *Pflaumann et al.* [2003]. As mentioned previously, in addition to an established open ocean source of SSA [*Monahan et al.*, 1986], we employ *Yang et al.*'s [2008, 2010] blowing snow source; see below for details. From the point of its production, the transport (and deposition) of SSA of different sizes (21 dry-particle-radius bins spanning 0.1–10 μm) is treated separately. Likewise, the transport (and deposition) of SSA from the open ocean, and from blowing snow, is treated separately. We thereby retain information on both the size and source of SSA. The SSA is transported (conserving sea salt sodium mass) in precisely the same way as trace gases are habitually transported in the model, using the second-order moments advection scheme of *Prather* [1986], coupled to the nonlocal vertical diffusion boundary layer scheme of *Holtslag and Boville* [1993] and *Tiedtke*'s [1989] parameterization of convection.

Following *Yang et al.* [2008], the flux of sea salt from blowing snow is derived from the blowing snow sublimation flux of *Déry and Yau* [1999, 2001]. Expressed in *Yang et al.*'s [2008] equations (1)–(5), the latter is indirectly a function of surface wind speed, air temperature, relative humidity, and snow age. The threshold 10 m wind speed above which snow is blown, for example, takes a reference value of 6.975 m s^{-1} but also depends on air temperature; see *Yang et al.* [2008, equation (2)]. Their equation (6) expresses the two-parameter gamma probability density function [*Budd*, 1966; *Schmidt*, 1982] governing the size distribution of blowing snow particles, and the snow-salinity measurements of *Massom et al.* [2001] are used to determine the mass of sea salt contained within each blowing snow particle. The latter is used to calculate the dry radius of SSA particle produced as each blowing snow particle sublimes and the SSA bin in which that mass of sea salt is transported. We include the production and transport of SSA particles up to a dry radius of 10 μm.

In view of the computational demands of running a global model at a resolution of 2.8° × 2.8° on 31 levels (stretching from the surface to 10 hPa) for a total of around 100 model years, and following the transport of 42 sea salt tracers (21 open ocean + 21 blowing snow), we adopt the relatively simple formulations for SSA deposition previously used by *Reader and McFarlane* [2003]. First, two exponential decays account for wet deposition by collision and nucleation scavenging: equations (1) and (2), respectively, combined in equation (3).

$$M_{L,r_{\mathrm{dry}},t+\Delta t} = M_{L,r_{\mathrm{dry}},t}\cdot \mathrm{e}^{-\alpha_{\mathrm{C}}\, PC_L\, \Delta t} \tag{1}$$

$$M_{L,r_{\mathrm{dry}},t+\Delta t} = M_{L,r_{\mathrm{dry}},t}\cdot \mathrm{e}^{-\alpha_{\mathrm{N}}\, PN_L\, \Delta t} \tag{2}$$

$$M_{L,r_{\mathrm{dry}},t+\Delta t} = M_{L,r_{\mathrm{dry}},t}\cdot e^{-\left(\alpha_{\mathrm{C}}\, PC_L + \alpha_{\mathrm{N}}\, PN_L\right)\Delta t} \tag{3}$$

At each model timestep ($\Delta t = 1800$ s), a fraction of the SSA in each dry-radius bin (r_{dry}), in each model box, on each model level (L), is removed based on scavenging parameters, α_{C} and α_{N} (units of kg^{-1} m^2), and the rates of precipitation originating in all levels above level L, PC_L (units of kgm^{-2} s^{-1}), and specifically in level L, PN_L (units of kgm^{-2} s^{-1}). α_{C} depends on the radius of SSA (r_{amb}) subject to fractional (cf. percentage) ambient relative humidity (H): $\alpha_{\mathrm{C}} = 0.2$ ($r_{\mathrm{amb}} < 0.5$ μm), 0.7 (0.5 μm $< r_{\mathrm{amb}} <$ 1.0 μm), and 1.2 ($r_{\mathrm{amb}} >$ 1.0 μm); we calculate r_{amb} based on r_{dry} and H, according to equation (4). $\alpha_{\mathrm{N}} = 2.3$ m^2 kg^{-1} [*Reader and McFarlane*, 2003].

$$r_{\mathrm{amb}} = r_{\mathrm{dry}}\cdot\{2/[0.016 - \ln(H)] + 1\}^{1/3} \tag{4}$$

Two deposition velocities account for dry deposition by sedimentation and turbulence: equations (5) and (6), respectively, combined serially in equation (7).

$$v_{\mathrm{stk}} = \left(0.22 g \rho_{\mathrm{s}} {r_{\mathrm{amb}}}^2\right)/\nu \tag{5}$$

$$u_{\mathrm{d}} = \left\{ (C_{\mathrm{D}}\cdot u)^{-1} + \left[\left({S_{\mathrm{C}}}^{-2/3} + 10^{-3/S_{\mathrm{t}}}\right)\cdot {C_{\mathrm{D}}}^{1/2}\cdot u\right]^{-1}\right\}^{-1} \tag{6}$$

$$v_{\mathrm{d}} = v_{\mathrm{stk}} + u_{\mathrm{d}} \tag{7}$$

with

$$C_{\mathrm{D}} = \left[k^{-1}\cdot \ln(h/z_0)\right]^{-2} \tag{8}$$

$$S_{\mathrm{t}} = \left(v_{\mathrm{stk}} C_{\mathrm{D}} u^2\right)/(g\,\nu) \tag{9}$$

The Stoke's velocity, v_{stk} (units of m s^{-1}), is calculated as a function of gravitational acceleration, $g = 9.81$ m s^{-2}; the density of SSA particles subject to ambient humidity, ρ_{S} (units of kg m^{-3}); their corresponding radius, r_{amb} (units of m); and atmospheric viscosity, $\nu = 1.79 \times 10^{-5}$kg m^{-1} s^{-1}. The turbulent dry deposition velocity, u_{d} (units of m s^{-1}), is calculated as a function of the dimensionless surface drag coefficient, C_{D}; the horizontal wind speed in the lowest level of the model, u (units of m s^{-1}); the dimensionless Schmidt number, S_{C}, assumed equal to 1.1×10^{12} r_{amb} (r_{amb} in units of m); and the dimensionless Stoke's number, S_{t}. C_{D} is calculated according to *SethuRaman and Raynor* [1975] in equation (8), as a function of the dimensionless von Kármán constant, $k = 0.4$; the height of the centre of the lowest model level, h (units of m); and the roughness length of the underlying surface, z_0 (units of m). We calculate S_{t} as a function of v_{stk}, C_{D}, u, g, and ν, according to equation (9). The resulting deposition velocity, v_{d} (units of m s^{-1}), is passed to the model's dry deposition scheme [*Giannakopoulos et al.*, 1999].

2.2. Model Tuning to Observations

We tune the model toward monthly mean sea salt concentration measurements at a variety of sites distributed widely around the globe, primarily those previously compiled by *Gong et al.* [2002] but supplemented with those reported by *Weller and Wagenbach* [2007] and *Jourdain et al.* [2008]. The solid red lines in Figure 1 illustrate the measured sea salt concentrations at the eight coastal sites previously explored by *Gong et al.* [2002]; see their Figure 7. Where possible, we have obtained the original measurements on which their Figure 7 was based and calculated not only the mean monthly mean sea salt concentrations but the standard deviations therein (the error bars in our Figure 1), which provide a measure of interannual variability. Where we omit error bars (Alert and Cape Grim), we have been unable to obtain the original measurements and have instead estimated the mean monthly mean concentrations from their Figure 7. Note that owing to a discrepancy at Neumayer between the scaling of the measurements reported by *Gong et al.* [2002] and that reported by the team that produced the data, we instead use 25 years of measurements spanning 1983 to 2005, the first 23 years of which were reported by *Weller and Wagenbach* [2007].

The measurements compiled by *Gong et al.* [2002] were predominantly made in the mid-1990s (see legends in Figure 1 for specific years) and inform our choice of years in which to explore the relative influences of interannual variations in sea ice extent and meteorology: 1990–1998. The dashed red lines in Figure 1 illustrate the sea salt concentrations that *Gong et al.* [2002] simulated with a general circulation model (GCM) and the open ocean source of *Monahan et al.* [1986]. They generally achieved good agreement between model and measurements at midlatitudes, while somewhat underestimating sea salt concentrations in the tropics and high latitudes. Reproducing observed sea salt concentrations is challenging, not least due to the highly nonlinear (roughly cubic) dependence of SSA production on wind speed that yields sea salt concentrations spanning several orders of magnitude. Notably, *Gong et al.* [2002] found that the wind speeds at the ocean surface simulated by their GCM were 18% higher than those in ECMWF analyses and necessary to capture the magnitude of observed sea salt concentrations. On the grounds that gustiness will not be captured in 6-hourly analyses, we similarly increase the ECMWF wind speeds in the lowest level of p-TOMCAT, with which we calculate the production of SSA, by a factor of 1.18; we do not, however, change the ECMWF winds with which the transport in the model is driven.

We also make minor changes to *Yang et al.*'s [2010] parameterization of the blowing snow source of SSA. We reduce the salinity of snow on sea ice by a factor of 2 on the grounds that the measurements on which it is based [*Massom et al.*, 2001] were made at a variety of snow depths. The salinity of snow on sea ice decreases with increasing depth of snow above the salty sea ice surface, and it is the uppermost snow that we expect to be blown. We also remove the 3.5-fold increase in snow salinities artificially applied to the northern hemisphere relative to the southern hemisphere. Owing to the uncertainties in modeled precipitation (see below), we remove spatial and temporal variability in snow age, setting this to a constant 5 days. The snow age affects the blowing snow sublimation flux [see *Yang et al.*, 2008]. Apart from the first 24 h, however, it has a modest influence, for instance, reducing the flux by 27% on increasing from 3 to 7 days.

Finally by way of tuning, again in view of the model's crude treatment of precipitation, we tune the rates of SSA wet deposition by multiplying PC_L and PN_L (used in equations (1)–(3); see section 2.1) by factors of 0.33, 0.75, and 3 in the low latitudes (45°N–45°S), midlatitudes (45°N–65°N and 45°S–65°S), and high latitudes (65°N–90°N and 65°S–90°S), respectively. Note that only the changes we make at middle and high latitudes affect the sea salt concentrations, we simulate in the polar regions. The small reduction (25%) at midlatitudes is necessary to broadly reproduce observed sea salt concentrations in this region; the increase at high latitudes is necessary to reproduce the observed gradient in sea salt concentration from coastal to central Antarctica (see below). *Giannakopoulos et al.* [2004] compared the precipitation in the model—an earlier version, but one employing the same treatment of precipitation—with two observational climatologies: *Jaeger* [1976] and *Legates and Willmott* [1990]. The two climatologies are not entirely consistent with each other in the middle and high southern latitudes; see *Giannakopoulos et al.* [2004, Figures 3 and 4]. However, *Giannakopoulos et al.* [2004] reported that compared to these climatologies, the model does not generate sufficient rainfall south of 30°S: 1–2 mm/day compared to the observed 2–5 mm/day—an underestimation by a factor of 2–3. This partly justifies the threefold increase in precipitation we artificially apply south of 65°S but not the reduction, albeit a small reduction (25%), between 45 and 65°S, or the abrupt change at 65°S. We

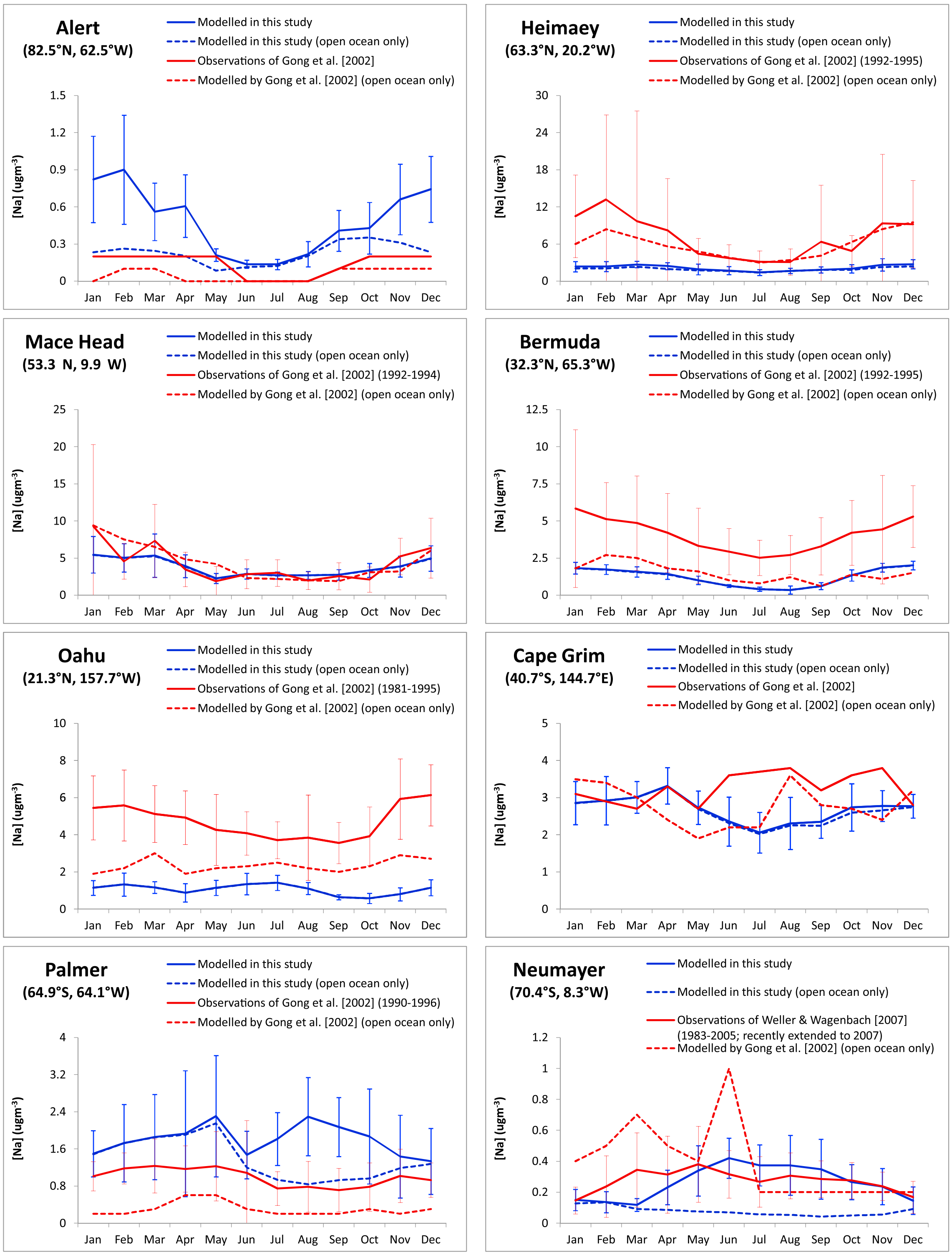

Figure 1. Comparison of mean (± 1σ) monthly mean sea salt concentrations modeled in this study with those based on measurements compiled by *Gong et al.* [2002] and reported by *Weller and Wagenbach* [2007]; see text for details.

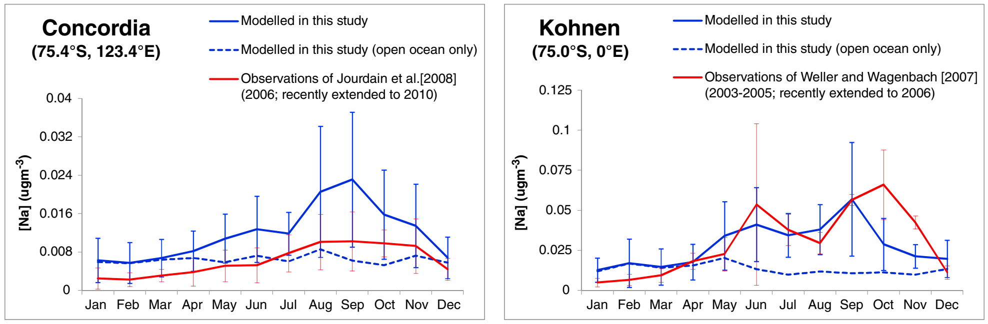

Figure 2. Comparison of mean (± 1σ) monthly mean sea salt concentrations modeled in this study with those based on measurements reported by *Jourdain et al.* [2008] and *Weller and Wagenbach* [2007]; see text for details.

also note that the model's underestimation of rainfall, compared to the climatologies, appears to be most pronounced in the midlatitudes. Our tuning via wet deposition is crude.

We could have achieved a similar gradient from coastal to central Antarctica by instead increasing the rates of dry deposition at high latitudes or a combination of wet and dry deposition rates. To verify that our findings are insensitive to the chosen means of tuning in this region, we repeat all experiments (described in the next section) subject to an alternative approach, in which we do not change PC_L or PN_L at high latitudes but instead increase the rates of dry deposition to snow and ice here by increasing the values of z_0 (used in equation (8); see section 2.1) by a factor of 250. The results to these repeat experiments are included in the supporting information. Importantly, though some of these differ quantitatively from the results presented in the main manuscript, they support the same qualitative conclusions, which we therefore regard as robust. We note that the need to slightly reduce deposition at midlatitudes, and increase it at high latitudes, could conceivably reflect an inaccuracy in model transport: too rapid uplift of SSA out of the boundary layer and hence too little deposition close to its sources and too much transport inland. A full investigation of how best to achieve agreement between the model and observations would be useful but is beyond the scope of the current study.

The sea salt concentrations that we simulate at the eight sites explored by *Gong et al.* [2002], after tuning the model, are illustrated in Figure 1 (solid blue lines). These are the mean (±1*σ*) monthly mean sea salt concentrations that we calculate in our 9 year BASE simulation (1990–1998) employing continuously varying sea ice extent (HadISST) and meteorology (ECMWF); the results to a preceding three month model spinup are not included. Like *Gong et al.* [2002], we underestimate the observations in the tropics (Oahu and Bermuda), but it is the southern middle and high latitudes that are responsible for the sea salt reaching Antarctic sites and hence relevant to this study. We reproduce well the observations at Cape Grim (41°S) while overestimating those at Palmer (65°S) by approximately a factor of 2. At Neumayer, we obtain very good agreement with the observations of *Weller and Wagenbach* [2007]. Overall, the tuned model reproduces observed sea salt concentrations in the southern middle and high latitudes well, both in seasonality and scale—spanning 2 orders of magnitude between Cape Grim and Neumayer and 3 when including observations at Concordia Station and Kohnen Station (see below). Note that subject to the alternative tuning explored as a sensitivity test (see above, with reference to the supporting information), we significantly underestimate the observations at Neumayer. This is difficult to explain since we continue to reproduce well the observations at Cape Grim, Palmer, Concordia Station, and Kohnen Station; see Figures S1 and S2 in the supporting information.

Figure 2, analogous to Figure 1, compares the mean (±1*σ*) monthly mean sea salt concentrations that we calculate in our BASE simulation with those based on observations at two Antarctic ice core sites: Concordia station (75°S, 123°E) and Kohnen station (75°S, 0°E), referred to simply as Concordia and Kohnen from here on. The approximate locations of these ice core sites are indicated in Figure 3. Note that the observations were not made during the 9 year period we have simulated, but they nevertheless serve to test the ability of our model to capture the correct scale and seasonality of sea salt concentrations. The measurements at Concordia—the site of the Dome C ice core—were made by M. Legrand, B. Jourdain, and S. Preunkert at the CESOA Observatory between 2006 and 2010; those made in 2006 were published by *Jourdain et al.* [2008].

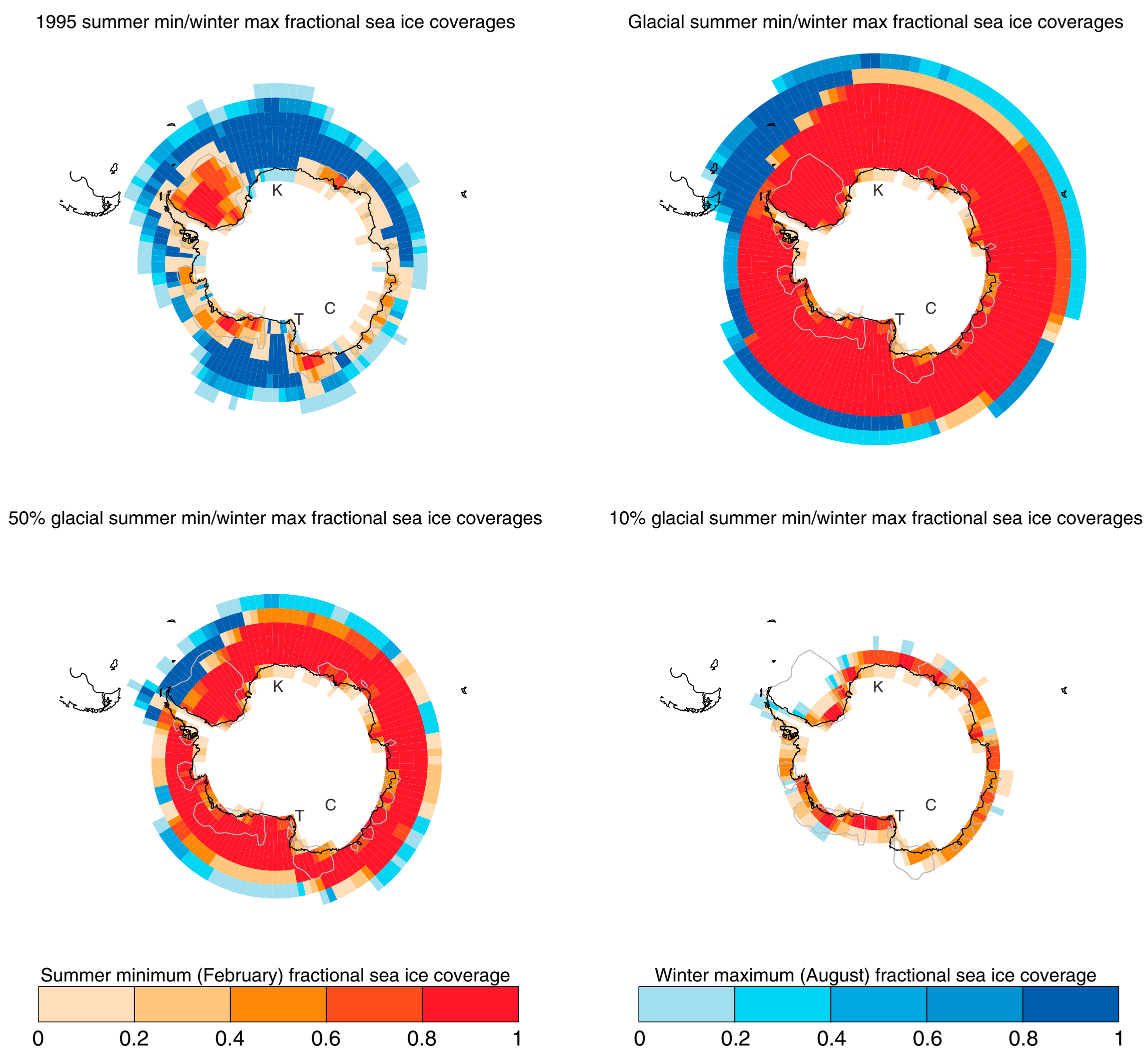

Figure 3. Summer minimum (February; red) and, beyond this, winter maximum (August; blue) fractional sea ice coverages in1995 and our glacial, 50% glacial, and 10% glacial sea ice scenarios; superimposed is the contour corresponding to a fractional sea ice coverage of 0.2 at the summer minimum (February; grey line) in 1995. The approximate locations of Concordia, Kohnen, and Taylor Dome are indicated by the letters C, K, and T, respectively.

The measurements at Kohnen—the site of the EDML ice core—were made via automatic year-round sampling of aerosol filters between 2003 and 2006; those made between 2003 and 2005 were published by *Weller and Wagenbach* [2007]. Since it is the measurements at Concordia that inform our tuning of the gradient in sea salt concentration from coastal to central Antarctica (discussed earlier), it is no coincidence that we reproduce reasonably well the scale of observed sea salt concentrations here. Ostensibly, they differ by about a factor of 2, however, the model and measurement periods (1990–1998 and 2006–2010, respectively) differ and the average measurements fall within the interannual variability exhibited by the model. We therefore do not further tune the model (e.g., by further increasing the precipitation south of 65°S). It is encouraging that we capture their seasonality. The measurements at Kohnen then provide an independent test of the model's ability to reproduce observations, and it appears we again capture well their scale and seasonality.

The dashed blue lines in this figure (and Figure 1) illustrate the sea salt concentrations we simulate as a result of the open ocean source of SSA alone. The difference between the dashed blue lines (open ocean) and solid blue lines (open ocean + blowing snow) illustrates the sea salt concentrations we simulate from blowing snow. It is interesting that at both sites, the seasonality (peaking in local winter) appears to be attributable to the blowing snow source. However, the relative contributions that the open ocean and blowing snow sources make to the total sea salt concentrations we simulate could be functions not only of the source parameterizations employed but also of the model tuning. New measurements are needed to experimentally constrain these contributions.

2.3. Sensitivity Experiments

To explore whether, on interannual timescales, sea ice extent or meteorology principally controls the concentration of sea salt reaching Antarctic ice core sites, we carry out two variations on the BASE simulation: ICE and MET. We have so far presented only the average monthly mean sea salt concentrations calculated in the BASE simulation, but what we are really interested in is the underlying interannual variability in these concentrations and how much of this variability is reproduced when we vary only the sea ice extent or only the meteorology. In ICE, we vary the sea ice extent between 1990 and 1998 but employ repeated years of 1995 meteorology. In MET, we vary the meteorology between 1990 and 1998 but employ repeated years of 1995 sea ice extent.

To explore the impact of switching from recent to glacial sea ice extent, we carry out two variations on the MET simulation: LGM1 and LGM2. As in MET, we continue to vary the meteorology between 1990 and 1998—LGM1 and LGM2 thus employ precisely the same, recent meteorology—but employ glacial sea ice extent (GLAMAP-based). LGM1 and LGM2 differ in their treatments of the additional sea ice under glacial conditions. In LGM1, we treat only the sea ice beyond the glacial summer minimum (the February field of the GLAMAP-based reconstruction; see section 2.1 for details) as a source of salty blowing snow, assuming the sea ice present at the summer minimum is too thick to be depressed under the weight of falling snow and hence too thick to be flooded by sea water and thereby make the snow on that sea ice salty; see section 1. This is an extension of the approach taken in BASE, ICE, and MET, in which only the sea ice beyond the recent summer minimum (the preceding February field of the HadISST data set) is treated as a source of salty blowing snow. Figure 3 illustrates the summer minimum (February; red) and, beyond this, winter maximum (August; blue) fractional sea ice coverages in 1995 (top left) and our glacial sea ice scenario (top right); superimposed on each is the contour corresponding to a fractional sea ice coverage of 0.2 at the summer minimum (February; grey line) in 1995. Note that relative to the diatom-based reconstruction of *Gersonde et al.* [2005, Figure 4], the GLAMAP-based reconstruction of glacial sea ice extent explored here considerably overestimates the glacial summer minimum sea ice coverage in the Pacific sector of the Southern Ocean.

In LGM2, we explore the consequences of treating much more of the glacial sea ice as a source of salty blowing snow—all sea ice beyond the 1995 summer minimum (approximated by the grey line in Figure 3). We do so not only because the diatom-based reconstruction of glacial sea ice extent shows much less summer sea ice in the Pacific sector (see above) but also because ship-based observations [*Worby et al.*, 2008, Figure 6a] reveal that in the annual mean, most Antarctic sea ice is relatively thin ($<$1 m and often $<$0.5 m) even in regions where sea ice is apparently present year round, such as in the Bellingshausen Sea. There are exceptions, such as the western Weddell Sea and the eastern Ross Sea, where thicker ice (1–2 m) is observed. However, these exceptional areas not withstanding, it is possible that even in regions where sea ice is observed year round, it is thin enough to be depressed under the weight of falling snow and ship-based observations show annual-mean snow cover of 0.1–0.2 m in these regions [*Worby et al.*, 2008, Figure 6b]. The sea ice observed year round in these regions may in fact be newly formed sea ice that we observe in transit as it is advected from its site of formation toward lower latitudes by katabatic winds. This would be consistent with the patterns and causes of sea ice drift recently reported by *Holland and Kwok* [2012], and we see no reason why, to first order, this should not extend to glacial sea ice, in which case much of that sea ice could be a source of salty blowing snow.

Finally, assuming the concentration of sea salt reaching Antarctic sites changes with sea ice extent, we explore how the sensitivity of this potential proxy varies as a function of it. The motivation for doing so stems from the observation that at each glacial termination, the ice core proxy for air temperature (δD) begins to change as much as around 2000 years before the flux of sea salt starts to change [*Röthlisberger et al.*, 2008]. It is possible that the extent of sea ice did not change for up to 2000 years after the climate began to change, but *Röthlisberger et al.* [2010] instead suggested that the flux of sea salt may simply be insensitive to the initial reduction in sea ice from its glacial extent, due to the very long transport time of SSA produced at the glacial northern sea ice edge [*Fischer et al.*, 2007a]. To explore this, we carry out a series of 1 year simulations, each employing precisely the same meteorology (1995) but a different fraction of the glacial (GLAMAP-based)

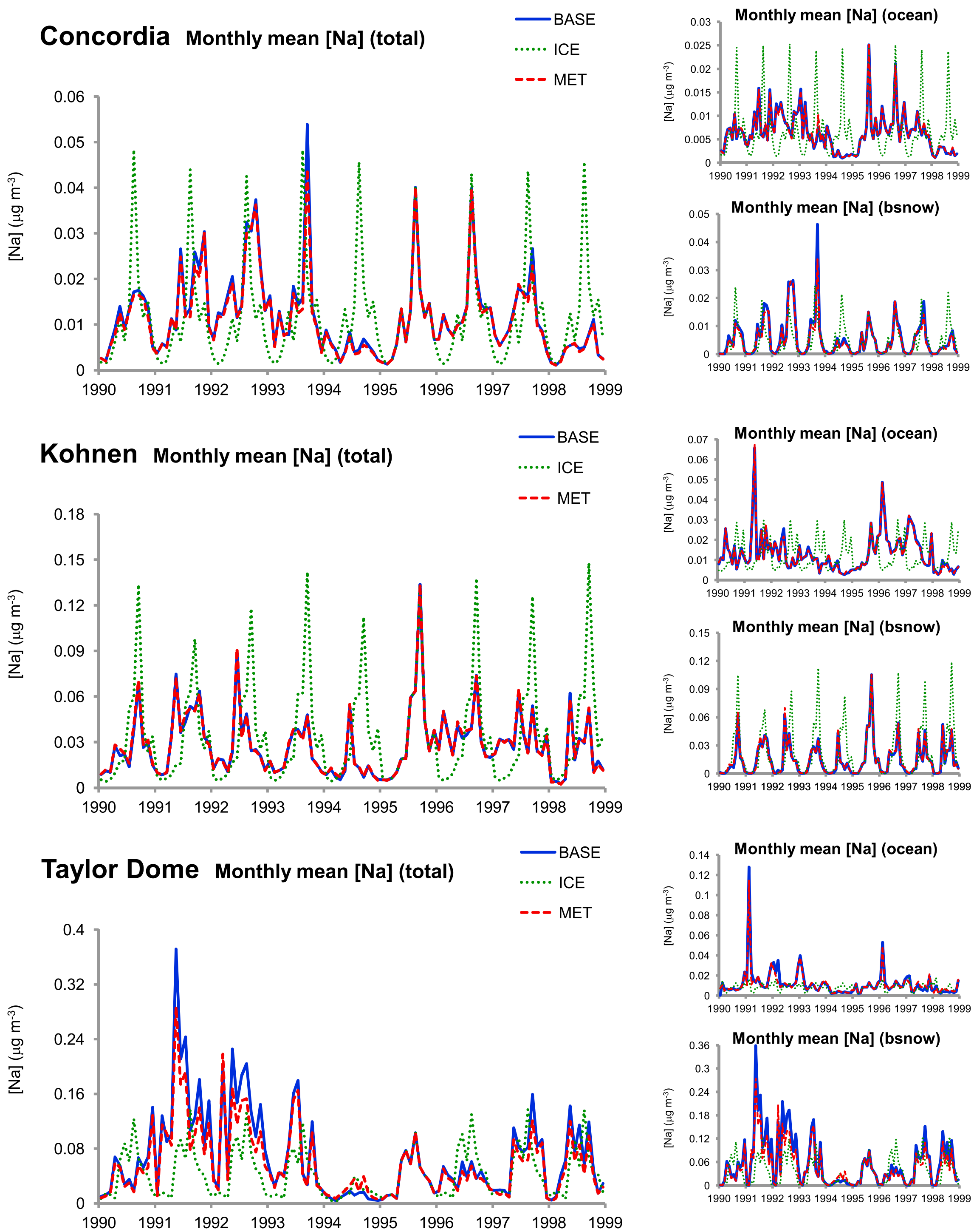

Figure 4. Monthly mean sea salt concentrations modeled in the BASE, ICE, and MET simulations at Concordia, Kohnen and Taylor Dome; see text for details.

sea ice extent: reduced from 100 to 10% in increments of 10% areal coverage (applied to each 2.8° longitudinal sector of the model, each month). We do so subject to treating (i) only the seasonal sea ice in each sea ice scenario and (ii) all sea ice beyond the 1995 summer minimum, as a source of salty blowing snow, similar to our treatments in LGM1 and LGM2, respectively (see above). The summer minimum (February; red) and, beyond this, winter maximum (August; blue) fractional sea ice coverages in our 50% and 10% glacial sea ice scenarios are illustrated in Figure 3. As before, superimposed on each is the contour corresponding to a fractional sea ice coverage at the summer minimum (February; grey line) in 1995. Note that these are artificial constructs; neither the 50% nor the 10% glacial sea ice scenario resembles recent sea ice extent, and the difference between the summer minimum and winter maximum sea ice coverages in the 10% scenario is negligible. We are mainly interested in what happens as we approach 100% glacial sea ice extent.

3. Results

In this section, we present detailed analysis of the sea salt concentrations we simulate at three Antarctic ice core sites, the approximate locations of which are indicated in Figure 3: Concordia (Dome C), Kohnen (EDML), and Taylor Dome. Where possible, we then extend our model analysis to the whole of Antarctica. We choose Concordia and Kohnen on the basis that we have observations of atmospheric concentration at these sites with which to compare our simulated sea salt concentrations; see section 2.2. We lack such observations at Taylor Dome, but it presents a particularly interesting site for comparison with Concordia, being much closer to the coast and, climatologically, broadly upwind. We expect to simulate higher sea salt concentrations here than at Concordia, and perhaps a greater contribution to total sea salt from the blowing snow source, due to its proximity to the Ross Sea, from which SSA transport timescales are much shorter and which has extensive winter sea ice.

3.1. Drivers of Interannual Variability

Figure 4 illustrates the nine years of monthly mean sea salt concentrations (1990–1998) we simulate at Concordia, Kohnen, and Taylor Dome in our BASE, ICE, and MET simulations; the results to each preceding 3 month model spinup are not shown. The BASE simulation (solid blue line) shows considerable interannual variability. The question is what drives this. When we continue to vary the sea ice extent throughout the 9 years but employ the same year of meteorology year on year (ICE; dashed green line), we reproduce very little of this interannual variability. At Concordia, for instance, we calculate a root-mean-square (RMS) percentage change in monthly mean sea salt concentrations in the ICE simulation relative to the BASE simulation of around 100%. When, on the other hand, we continue to vary the meteorology throughout the 9 years, but employ the same year of sea ice extent year on year (MET; dashed red line), we reproduce practically all of the interannual variability: we calculate an RMS percentage change in monthly mean concentrations in MET relative to BASE of about 5%. This holds irrespective of whether we look at total simulated sea salt concentrations or the concentrations stemming solely from the open ocean or blowing snow. We conclude that the interannual variability in the sea salt concentrations we simulate at Concordia is almost exclusively driven by interannual variability in meteorology, and we reach the same conclusion at Kohnen and Taylor Dome. Note that the “meteorology” includes multiple factors affecting the sea salt concentrations we simulate: the winds governing SSA production at the open ocean and sea ice surfaces, the winds governing SSA transport to each site, and the precipitation governing the rate of SSA wet deposition en route. However, the key message is that meteorology, not sea ice extent, drives interannual variability in our model.

Figure 5 illustrates the RMS percentage changes in monthly mean sea salt concentrations in the ICE simulation (top) and the MET simulation (bottom), relative to the BASE simulation, across the surface of Antarctica. We find that the meteorology proves the dominant influence on the total sea salt concentration we simulate across almost the entire continent, with the RMS percentage change in MET relative to BASE being typically less than 20% and less than a fifth (often less than a tenth) of the RMS percentage change in ICE relative to BASE, typically greater than 100%. We obtain a still more resolute picture regarding sea salt solely from the open ocean: the meteorology is clearly the dominant influence. The picture regarding sea salt from blowing snow, however, is more balanced: both sea ice extent and meteorology are influential, as evidenced by substantial RMS percentage changes in both MET and ICE, relative to BASE: 20–80% and 100–200%, respectively. Around much of the Antarctic coast and the Antarctic Peninsula, the RMS percentage change in MET is actually similar to, or greater than, that in ICE. Here, close to regions of blowing snow, sea ice extent is an important factor in determining the concentration of sea salt we simulate from that source. Note, however, that our simulations still suggest that meteorology, not sea ice extent, predominantly controls the total sea salt concentration in these regions.

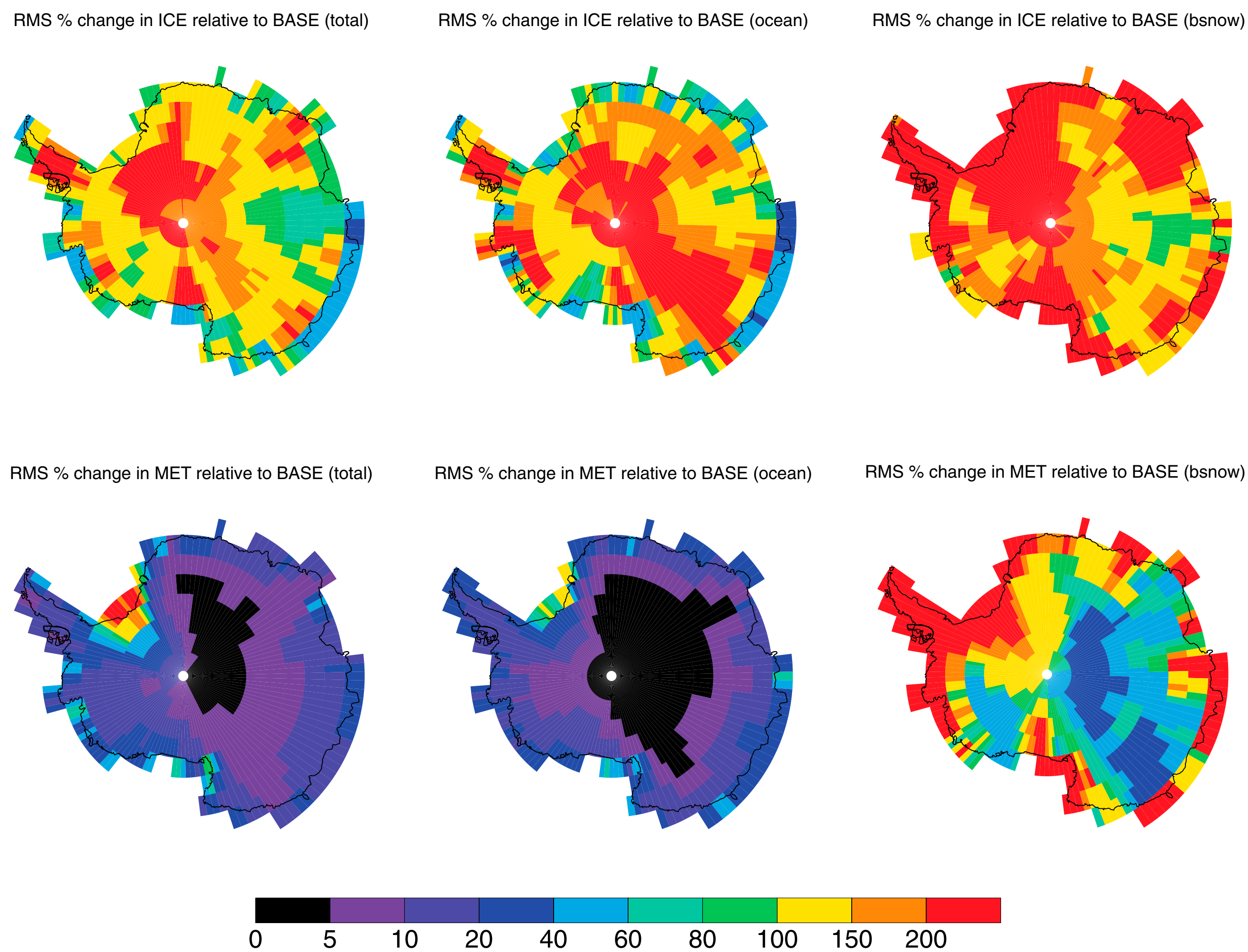

Figure 5. Root-mean-square (RMS) percentage changes in monthly mean sea salt concentrations simulated across the surface of Antarctica in (top) ICE and (bottom) MET, relative to BASE. The changes in total sea salt concentration are illustrated on the left, with the changes in the concentration of sea salt solely from the open ocean and solely from blowing snow on sea ice in the middle and on the right, respectively; see text for details.

3.2. Impact of Glacial Sea Ice Extent

Figure 6 illustrates the 9 years of monthly mean sea salt concentrations (1990–1998) we simulate at Concordia, Kohnen, and Taylor Dome in our MET, LGM1, and LGM2 simulations; the results to each preceding 3 month model spinup are not shown. All three simulations employ precisely the same meteorology (1990–1998) but differ with regard to the sea ice extent they employ and/or how much of that sea ice is treated as a source of salty blowing snow (see section 2.3). The impact of switching from recent sea ice extent (MET; solid blue lines) to glacial sea ice extent (LGM1 and LGM2; dashed red and green lines respectively) appears to depend strongly on the latter.

If we treat only the glacial sea ice beyond the LGM summer minimum as a source of salty blowing snow (LGM1), we simulate lower sea salt concentrations at Concordia, both from the open ocean and from blowing snow: we calculate a mean percentage change in total monthly mean sea salt concentrations of −65%. This is not surprising as we are effectively adding a hinterland of benign sea ice and moving the blowing snow and open ocean sources of SSA away from central Antarctica. Much the same applies at Kohnen and Taylor Dome. Note that in the Pacific sector of the Southern Ocean, our GLAMAP-based glacial sea ice field considerably overestimates the glacial summer minimum in sea ice coverage featured in the diatom-based reconstruction of *Gersonde et al.* [2005] (see section 2.3). It is possible, therefore, that subject to treating only sea ice beyond the LGM summer minimum as a source of salty blowing snow, we overestimate the reduction in sea salt from blowing snow on switching to glacial sea ice extent.

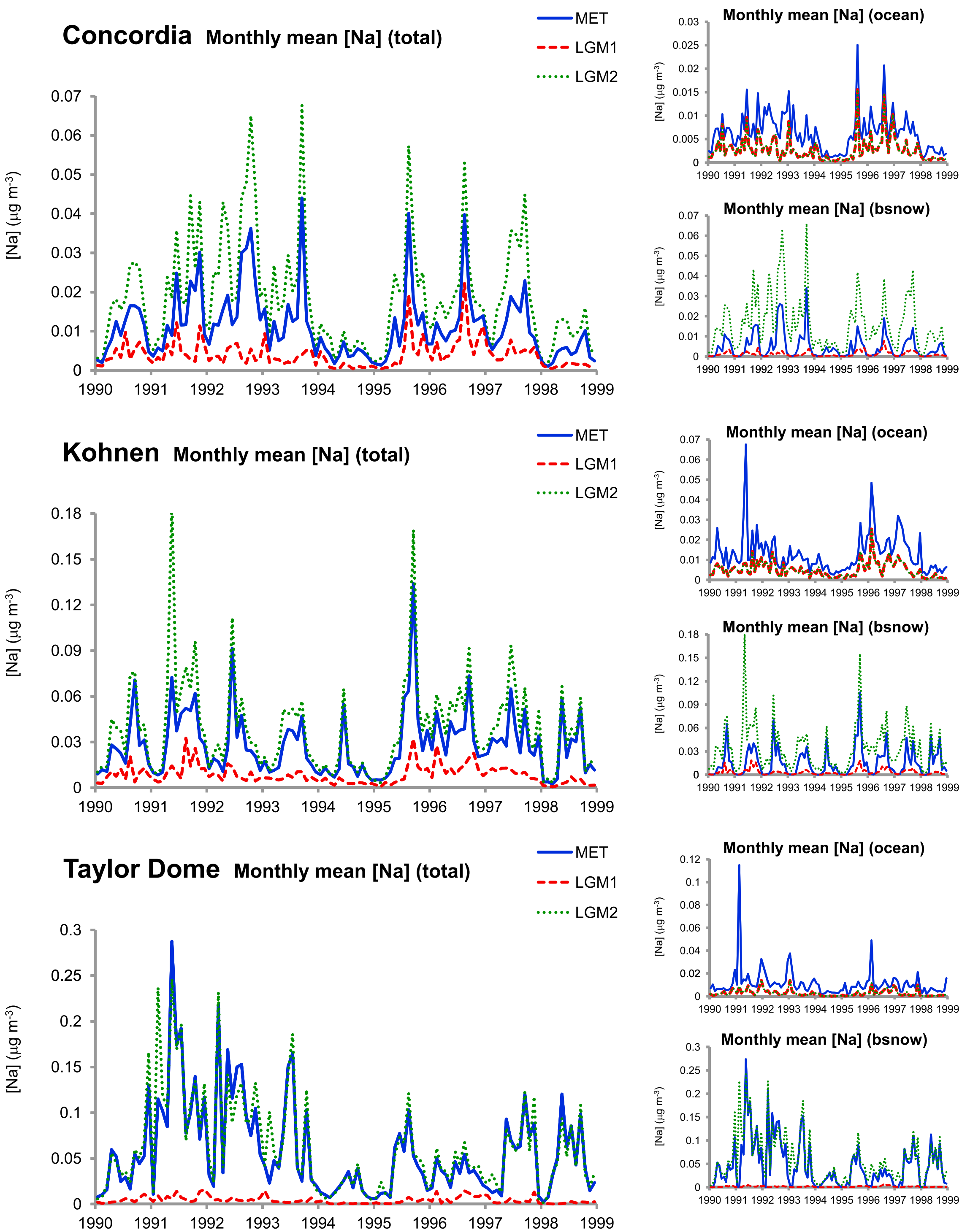

Figure 6. Monthly mean sea salt concentrations modeled in the MET, LGM1, and LGM2 simulations at Concordia, Kohnen, and Taylor Dome; see text for details.

When we instead treat all glacial sea ice beyond the recent summer minimum as a source of salty blowing snow (LGM2), the switch to glacial sea ice extent yields significantly higher total sea salt concentrations at Concordia: we calculate a mean percentage change in total monthly mean sea salt concentrations of +68%. The concentrations of sea salt we simulate from the open ocean are reduced to the same extent as in LGM1, as a result of the addition of sea ice and the movement of the open ocean source of SSA away from central Antarctica. However, the additional sea ice is now assumed to be a source of salty blowing snow, and the increase in sea salt we simulate from this source more than compensates for the reduction in sea salt we simulate from the open ocean. In other words, just replacing a region of open ocean with sea ice acting as a source of salty blowing snow yields an increase in the total concentration of sea salt we simulate reaching Concordia. We can thus explain much of the approximate twofold glacial increase in sea salt flux recorded in the Dome C ice core [*Wolff et al.*, 2006, 2010] without invoking a change in meteorology, such as increased storminess. Of course, increased storminess, driving increased SSA production and transport, and/or colder drier conditions, yielding longer SSA lifetimes with respect to wet deposition, could contribute to the further 20% increase in sea salt concentration implied by an approximate twofold increase in sea salt flux. At Kohnen, we also simulate an increase in sea salt from blowing snow that more than compensates for a reduction in sea salt from the open ocean, but one that results in a mean percentage increase in total monthly mean sea salt concentrations of only 42% compared to the near threefold increase in sea salt flux recorded in the EDML ice core [*Fischer et al.*, 2007b]. At Taylor Dome, we calculate a mean percentage increase of just 8% and it would be interesting to see how much higher the sea salt flux recorded in the ice here was at the LGM; *Steig et al.* [2000] report only a large increase in sea salt concentration (in ice) here. We do not place great importance on the absolute numbers; they differ, for instance, subject to the alternative tuning at high latitudes explored in the supporting information: we calculate mean percentage changes of +108%, +60%, and +74% at Concordia, Kohnen, and Taylor Dome, respectively. What is important, however, is that in the absence of any change in meteorology, just the increase in sea ice extent under glacial conditions yields a substantial increase in the concentration of sea salt we simulate reaching Antarctic sites. The 68% increase in atmospheric concentration we simulate at Concordia, in particular, could explain much of the approximate twofold increase in sea salt flux recorded in the Dome C ice core.

Note that in LGM2, as well as BASE, MET, and ICE, we are still assuming that sea ice present in the preceding February (i.e., apparently present year round) is too thick to yield salty blowing snow. For the reasons outlined in section 2.3, it is possible that much of this sea ice is in fact newly formed sea ice, observed in transit as it as advected from its site of formation toward lower latitudes by katabatic winds; ship-based observations suggest it is sufficiently thin (<1 m and often <0.5 m) to be depressed by the weight of snow falling on it (0.1–0.2 m) [see *Worby et al.*, 2008, Figure 6]. It is therefore possible that we somewhat underestimate the size of the blowing snow source of SSA subject to both recent and glacial sea ice extent.

Figure 7 illustrates the mean percentage changes in monthly mean sea salt concentrations that we simulate in the LGM1 and LGM2 simulations, relative to the MET simulation, across the surface of Antarctica. Generally, the findings at Concordia, Kohnen, and Taylor Dome extend to the rest of the continent. In LGM1, we calculate a substantial reduction in monthly mean total sea salt concentrations across Antarctica (25–100%), as a result of a reduction at all locations in SSA simulated from the open ocean and a fairly widespread reduction in SSA simulated from blowing snow. Note, however, that we calculate increases in the monthly mean concentration of sea salt from blowing snow at sites on the Antarctic Peninsula and in some parts of East and West Antarctica. The increase on the Peninsula (greatest at its northernmost tip) is presumably the result of moving the region of seasonal sea ice, treated as the source of salty blowing snow, northward. The modest increases in East and West Antarctica, however, are more difficult to explain. Ultimately, they must be the result of increased coincidence between regions of apparently seasonal sea ice, treated as a source of salty blowing snow, and regions of higher wind speeds, which drive greater SSA production and/or faster transport inland.

In LGM2, we calculate a substantial increase in monthly mean total sea salt concentrations across much of Antarctica (25–100%), similar to Concordia and Kohnen, with generally more modest increases around the coast (0–25%), similar to Taylor Dome. The widespread continental increase is attributable to an increase in the sea salt we simulate from blowing snow that more than compensates for the reduction in sea salt we simulate from the open ocean. The key message here is that the impact of switching from recent to glacial sea ice extent depends on how much of the glacial sea ice is a source of salty blowing snow but that should this be a large fraction, we can partially explain the glacial increase in sea salt fluxes recorded in central Antarctic cores, such as Vostok [*Petit et al.*, 1999], Dome C [*Wolff et al.*, 2006, 2010], and Dome Fuji [*Sato et al.*, 2013], without changing the meteorology. Just the replacement of some of the open ocean with sea ice drives a significant increase in the concentration of sea salt we simulate reaching Antarctic sites, including an increase at Concordia that could explain much of the approximate twofold increase in sea salt flux recorded in the Dome C ice core.

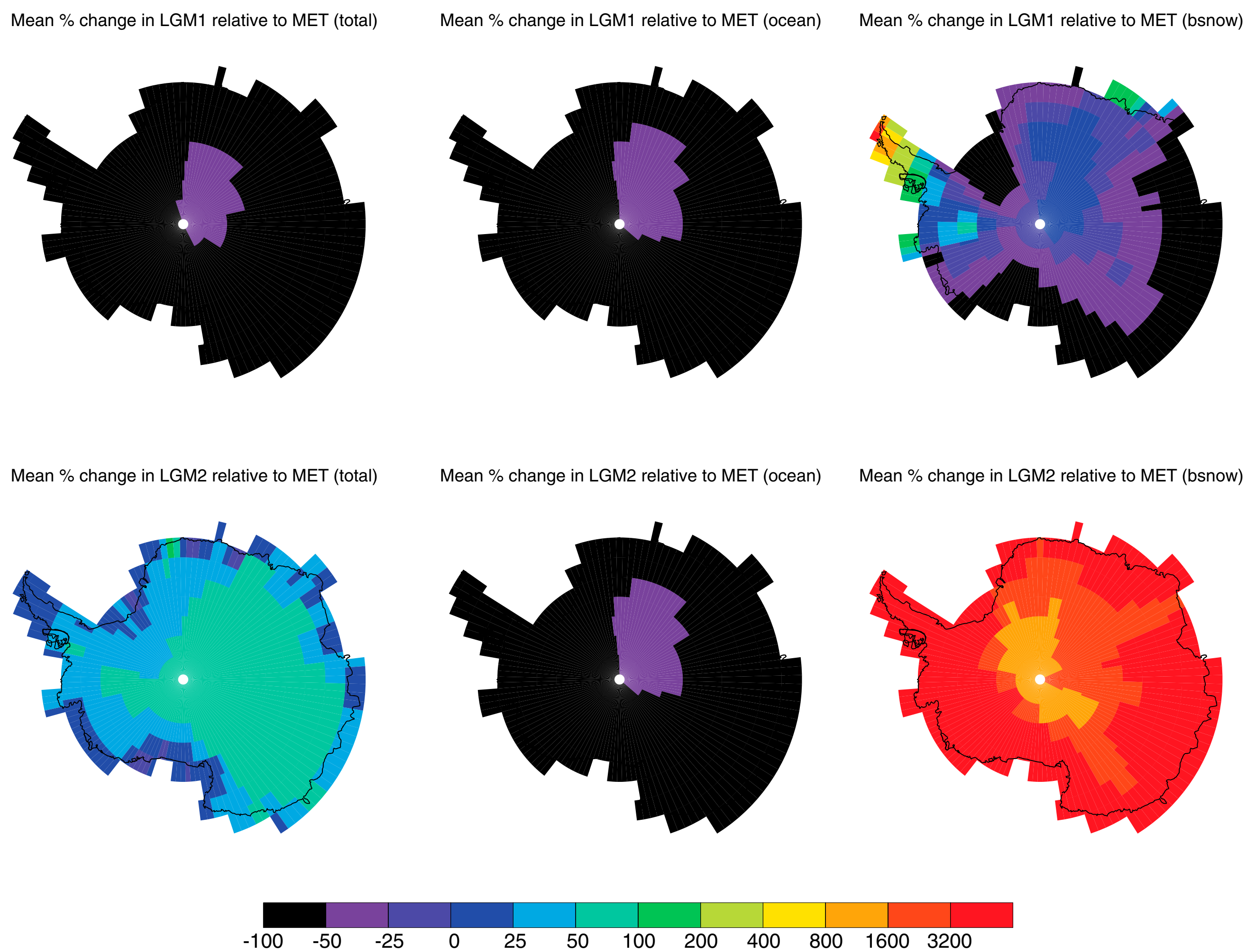

Figure 7. Mean percentage changes in the monthly mean sea salt concentrations simulated in the (top) LGM1 and (bottom) LGM2 simulations, relative to the MET simulation, across the surface of Antarctica; see text for details.

3.3. Sensitivity as a Function of Extent

Figure 8 illustrates the annual-mean sea salt concentrations we simulate at Concordia, Kohnen, and Taylor Dome in a series of 1 year simulations, employing precisely the same meteorology but different fractions of glacial sea ice extent (in terms of areal coverage; see section 2.3); the results to each preceding 3 month model spinup are not shown. Subject to treating only the seasonal sea ice in each scenario as a source of salty blowing snow (similar to LGM1; Figure 8, left), we find that the annual-mean total sea salt concentration we simulate at each site decreases with increasing sea ice extent. We would expect a reduction, as a result of moving the open ocean and blowing snow sources of SSA away from central Antarctica. It may therefore appear surprising that at each site we simulate an overall increase in the concentration of sea salt from blowing snow from 10% to around 70% glacial sea ice extent (while treating only the seasonal sea ice as a source of salty blowing snow). This is likely a product of the way we have artificially constructed the fractional glacial sea ice scenarios (see section 2.3); the very low sea salt concentrations attributable to blowing snow at 10% glacial sea ice extent (at Concordia and Taylor Dome in particular) reflect the negligible difference between summer minimum and winter maximum sea ice coverages in this scenario (see Figure 3 and text in section 2.3). The growing region of seasonal sea ice may, in addition, encounter stronger winds as it moves toward lower latitudes, driving greater SSA production from blowing snow and/or faster transport to the three sites. The result is nevertheless a reduction in annual-mean total sea salt concentration with increasing sea ice extent, as a result of a substantial reduction in sea salt from the open ocean.

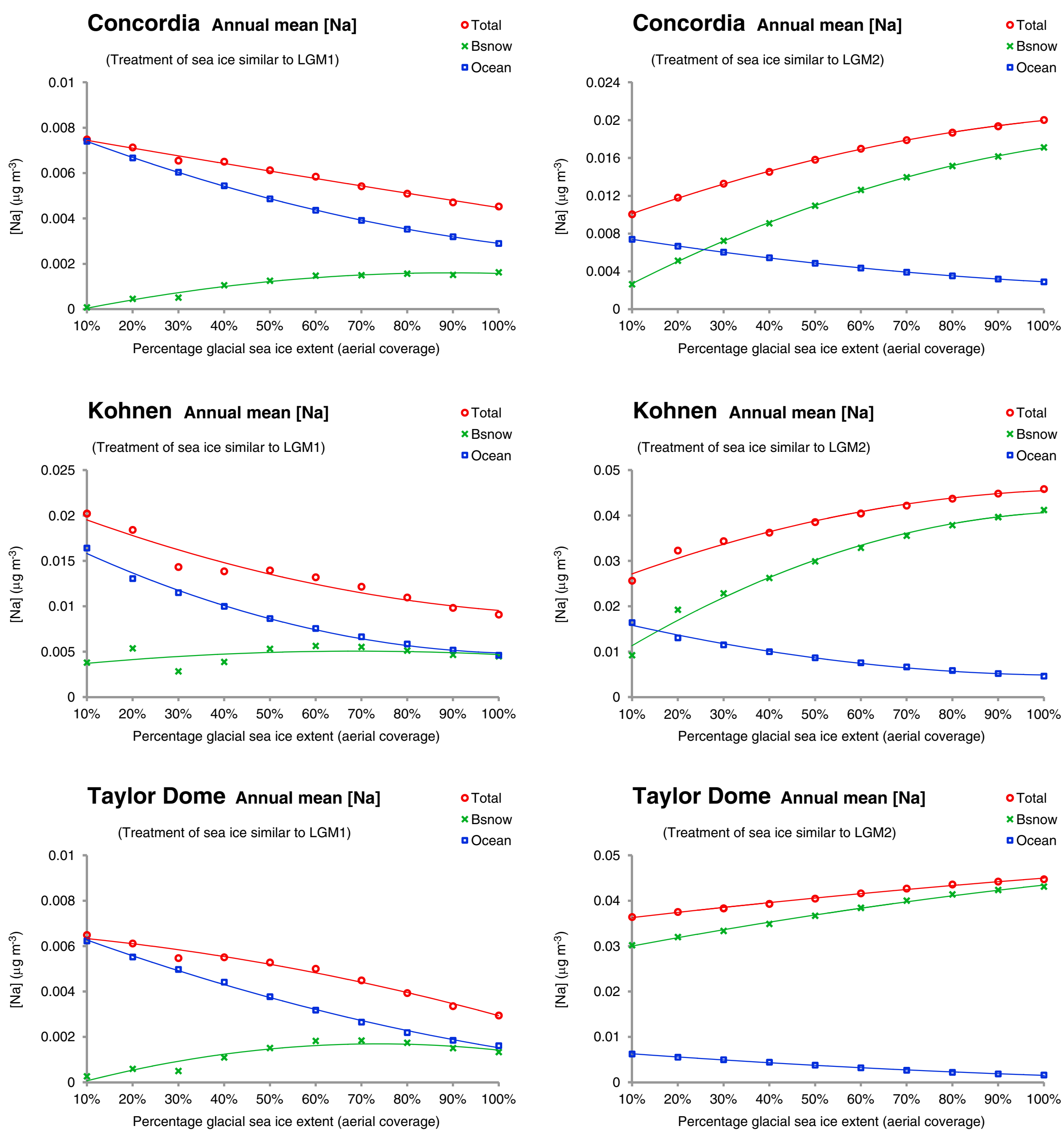

Figure 8. Annual-mean sea salt concentrations modeled at Concordia, Kohnen, and Taylor Dome in a series of 1 year simulations employing precisely the same meteorology in each but different fractions of glacial sea ice extent; see text for details.

When, in each scenario, we treat all sea ice beyond the recent summer minimum as a source of salty blowing snow (similar to LGM2; Figure 8, right), we simulate an increase in the annual-mean total sea salt concentration at each site with increasing sea ice extent. The sea salt from the open ocean decreases precisely as before, as a result of moving the open ocean source of SSA away from central Antarctica. However, we now simulate an increase in the annual-mean concentration of sea salt from blowing snow that more than compensates for this (consistent with the findings of the last section). What is particularly interesting, however, is that the increase in total sea salt concentration at each site, particularly at Concordia and Kohnen, appears to tail off as we approach 100% glacial sea ice extent. In other words, the annual-mean total sea salt concentration shows the smallest sensitivity to change in sea ice extent at the glacial end of the range of sea ice scenarios explored. Should much of the sea ice under glacial conditions have been a source of salty blowing snow, we may be able to explain not only why central Antarctic ice cores exhibit glacial maxima in sea salt flux but also why a lag is observed between δD starting to change, and sea salt flux beginning to change, at each termination [*Röthlisberger et al.*, 2008]: the sea salt proxy may simply be insensitive to the initial reduction in sea ice from its glacial extent [*Röthlisberger et al.*, 2010].

4. Summary and Discussion

We have used the Cambridge p-TOMCAT model of atmospheric chemistry and transport—including the process-based production, transport, and deposition of SSA from the open ocean [*Monahan et al.*, 1986] and blowing snow on sea ice [*Yang et al.*, 2008, 2010]—to explore the potential of sea salt as an ice core proxy for past sea ice extent. Specifically, we have explored whether, on interannual timescales, sea ice extent or meteorology principally controls the atmospheric concentration of sea salt reaching Antarctic sites, what impact switching from recent to glacial sea ice extent has on that, and how the sensitivity of this potential proxy varies as a function of sea ice extent.

Subject to current climate conditions, on interannual timescales, we find that meteorology, not sea ice extent, is the dominant control on the atmospheric concentration of sea salt we simulate at Antarctic sites—both coastal and continental (see section 3.1). It is possible that in the 9 years explored (1990–1998), the meteorology simply shows greater interannual variability than the sea ice extent and thus exerts greater influence. However, our findings are consistent with *Abram et al.*'s [2013] summation that interannual variations in sea ice extent exert a smaller influence on the sea salt reaching Antarctic sites, on a year to year basis, than variations in other factors such as transport patterns and the occurrence of polynyas. In our idealized model experiments, the "meteorology" includes multiple factors affecting the concentrations of sea salt we simulate: the wind speeds, air temperatures, and humidities governing the production of SSA; the strength and direction of winds governing its subsequent transport; and the precipitation governing its wet deposition en route. We intend, in a subsequent model study, to differentiate between the influences of the winds at source and the winds governing subsequent transport. Linked to that, we mean to explore from what regions of the Southern Ocean the sea salt reaching different Antarctic sites predominantly comes. We also plan on exploring what drives the seasonality in atmospheric sea salt concentrations in Antarctica (peaking in local winter) since even our simulation employing the same year of sea ice extent, year on year, includes an annual cycle in sea ice coverage. It will be interesting to see whether the dominant control of the "meteorology" on interannual timescales extends to seasonal ones.

The next question is what happens to the concentration of sea salt we simulate at Antarctic sites if, in the absence of any change in meteorology, we substantially change the sea ice extent. We find that the impact of switching from recent to glacial sea ice extent depends strongly on how much of the glacial sea ice we assume constitutes a source of salty blowing snow (see section 3.2). If only the seasonal sea ice is treated as such a source, we simulate a substantial reduction in total sea salt concentration across Antarctica (25-100%). When we instead treat all glacial sea ice beyond the recent summer minimum as such, we simulate a substantial increase in total sea salt concentration across much of Antarctica (25–100%), with more modest increases toward the coast (0–25%).

This is the first time that subject to a glacial scenario, a substantial increase in the supply of sea salt to Antarctica has been simulated in a process-based fashion (and in the absence of any change in meteorology). Previous model studies [*Genthon*, 1992; *Reader and McFarlane*, 2003; *Mahowald et al.*, 2006] simulated the atmospheric circulation subject to glacial boundary conditions and explored its consequences for the production, transport, and deposition of SSA. Employing only an open ocean source of SSA, *Genthon* [1992] found that changes in the strength of winds at source and changes in the efficiency of transport to Antarctica were insufficient to overcome the reduction in sea salt supplied as a result of the increased distance it had to travel over more extensive sea ice. Similarly, *Reader and McFarlane* [2003] could not explain the increased deposition of sea salt at the LGM, evident from ice core records. Notably, however, they found that the factor by which they underestimated this was reduced from approximately 10 to roughly 7 on including a simple (non-process-based) sea ice source of SSA. *Mahowald et al.* [2006] were also unable to simulate the necessary increase in sea salt deposition despite extending their open ocean source of SSA to regions of sea ice. New to the present study is the inclusion of a process-based sea ice source of SSA that proves a stronger source than the open ocean the sea ice replaces, namely, blowing snow on sea ice [*Yang et al.*, 2008, 2010].

This source has yet to be fully constrained by field measurements but, subject to the current parameterization, could yield a significant increase in total atmospheric sea salt concentration reaching central Antarctic sites, including a 68% increase at Concordia that could explain much of the approximate twofold increase in sea salt flux recorded in the Dome C ice core [see *Wolff et al.*, 2006, 2010]. (At a site of low snow accumulation rate, a twofold increase in sea salt flux implies roughly a twofold, or 100%, increase in atmospheric concentration.) We note, however, that we simulate this subject to (i) our proposition that much of the sea ice under glacial conditions could have been a source of salty blowing snow (for reasons outlined in section 2.2) and (ii) recent meteorology (see later). We would expect the increase in SSA lifetimes with respect to wet deposition, under colder, drier glacial conditions, to add to this increase. One of the next steps must be to explore the supply of sea salt to Antarctica under glacial conditions with a GCM employing both the blowing snow and open ocean sources of SSA.

It is also interesting that subject to treating much of the glacial sea ice as a source of salty blowing snow, we find that the total sea salt concentration we simulate at Concordia and Kohnen—the sites of the Dome C and EDML ice cores respectively—increases with increasing sea ice extent but shows the smallest sensitivity to change in sea ice extent at the glacial extreme (see section 3.3). This broadly supports *Röthlisberger et al.*'s [2010] proposed explanation for the lag observed between δD starting to change and sea salt flux beginning to change at each glacial termination [*Röthlisberger et al.*, 2008]. It is possible that sea ice extent began to decrease at the same time as air temperatures started to rise, and the sea salt proxy was simply insensitive to initial retreat.

If we now turn this exploration around and consider the potential to infer a change in sea ice extent from a change in sea salt flux recorded in an Antarctic ice core, there remains one challenge. Our simulations demonstrate that while changes in sea ice extent affect the amount of sea salt reaching Antarctic sites, so do changes in meteorology, at least on interannual timescales. It is straightforward to remove the influence of interannual variations in meteorology by measuring the average sea salt flux recorded in a length of core representative of 100 or 1000 years. However, to infer a change in sea ice extent from a change in sea salt flux, we will still need to know if and how the climatological meteorology changed. This may or may not prove straightforward. It is possible, for instance, that though it was colder and there was less precipitation at high latitudes under glacial conditions, as evidenced by measurements of δD and accumulation rate, respectively, the pattern of the winds governing the production and transport of SSA differed little from that at present. A recent comparison of the Talos Dome and Dome C ice core records of dust suggests the patterns of transport between these sites changed little over the whole of the last glacial-interglacial cycle [*Schüpbach et al.*, 2013], though of course the routes of dust and sea salt transport could in principle differ. If the climatological circulation changed little, or any changes therein can be constrained with observations, sea salt could provide an ice core proxy with which to obtain continuous long-term, regionally integrated records of sea ice extent to complement the site-specific records based on diatoms and emerging sea ice biomarkers.

Acknowledgments
This study is part of the British Antarctic Survey Polar Science for Planet Earth Programme and a contribution to the Past4Future and BLOWSEA projects funded, respectively, by the European Commission (7th Framework Programme) and the UK Natural Environment Research Council; we gratefully acknowledge their support. James Levine also acknowledges the support of the NERC-funded project, CLAIRE-UK, during preparation and revision of this manuscript, Xin Yang thanks NCAS-Climate for their support, and Eric Wolff acknowledges the Royal Society. We are grateful to the Centre for Atmospheric Science, University of Cambridge, for use of the Cambridge p-TOMCAT model, Cathy Reader of Environment Canada for her help in implementing simple treatments of SSA wet and dry deposition, and Louise Sime and Peter Frettwell of the British Antarctic Survey for their help, respectively, in utilizing GLAMAP SSTs and a high-resolution land/sea mask. We thank: Sunling Gong of Environment Canada for the sea salt concentration data underpinning Figure 7 of *Gong et al.* [2002]; Michel Legrand, Bruno Jourdain, and Susanne Preunkert of the Laboratoire de Glaciologie et Géophysique de l'Environnement for their sea salt measurements at the CESOA Observatory at Concordia Station; and Rolf Weller of the Alfred Wegner Institute and Dietmar Wagenbach of the Institut für Umweltphysik, University of Heidelberg, for the measurements at Kohnen Station and Neumayer. We are grateful to Paul Holland, Liz Thomas, and Tom Bracegirdle of the British Antarctic Survey for helpful discussions in the preparation of this manuscript. Finally, we thank two anonymous reviewers for their constructive comments and criticisms.

References

Abbatt, J. P. D., et al. (2012), Halogen activation via interactions with environmental ice and snow in the polar lower troposphere and other regions, *Atmos. Chem. Phys.*, *12*(14), doi:10.5194/acp-12-6237-2012.

Abram, N. J., E. W. Wolff, and M. A. J. Curran (2013), A review of sea ice proxy information from polar ice cores, *Quat. Sci. Rev.*, *79*, doi:10.1016/j.quascirev.2013.01.011.

Belt, S. T., and J. Müller (2013), The Arctic sea ice biomarker IP25: A review of current understanding, recommendations for future research and applications in palaeo sea ice reconstructions, *Quat. Sci. Rev.*, *79*, doi:10.1016/j.quascirev.2012.12.001.

Belt, S. T., G. Masse, S. J. Rowland, M. Poulin, C. Michel, and B. LeBlanc (2007), A novel chemical fossil of palaeo sea ice: IP25, *Org. Geochem.*, *38*, 16–27.

Brunke, M. A., M. Y. Zhou, X. B. Zeng, and E. L. Andreas (2006), An intercomparison of bulk aerodynamic algorithms used over sea ice with data from the Surface Heat Budget for the Arctic Ocean (SHEBA) experiment, *J. Geophys. Res.*, *111*, C09001, doi:10.1029/2005JC002907.

Budd, W. F. (1966), The drifting of nonuniform snow particles, in *Studies in Antarctic Meteorology*, *Antarct. Res. Ser.*, vol. 9, edited by M. J. Rubin, pp. 59–70, AGU, Washington, D. C.

Criscitiello, A. S., S. B. Das, M. J. Evans, K. E. Frey, H. Conway, I. Joughin, B. Medley, and E. J. Steig (2013), Ice-sheet record of recent sea-ice behaviour and polynya variability in the Amundsen Sea, West Antarctica, *J. Geophys. Res. Oceans*, *118*, 118–130, doi:10.1029/2012JC008077.

Déry, S. J., and M. K. Yau (1999), A bulk blowing snow model, *Boundary Layer Meteorol.*, *93*, 237–251.

Déry, S. J., and M. K. Yau (2001), Simulation of blowing snow in the Canadian Arctic using a double-moment model, *Boundary Layer Meteorol.*, *99*, 297–316.

Erickson, D. J., III, J. T. Merrill, and R. A. Duce (1986), Seasonal estimates of global atmospheric sea-salt distributions, *J. Geophys. Res.*, *91*, 1067–1072.

Fischer, H., M.-L. Siggaard-Andersen, U. Ruth, R. Röthlisberger, and E. Wolff (2007a), Glacial/interglacial changes in mineral dust and sea-salt records in polar ice cores: Sources, transport and deposition, *Rev. Geophys.*, *45*, RG1002, doi:10.1029/2005RG000192.

Fischer, H., et al. (2007b), Reconstruction of millennial changes in dust emission, transport and regional sea ice coverage using the deep EPICA ice cores from the Atlantic and Indian Ocean sector of Antarctica, *Earth Planet. Sci. Lett.*, *260*(1–2), 340–354.

Genthon, C. (1992), Simulations of desert dust and sea salt aerosols in Antarctica with a general circulation model of the atmosphere, *Tellus*, *44B*, 371–389.

Gersonde, R., X. Crosta, A. Abelmann, and L. Armand (2005), Sea-surface temperature and sea ice distribution of the Southern Ocean at the EPILOG Last Glacial Maximum—A circum-Antarctic view based on siliceous microfossil records, *Quat. Sci. Rev.*, *24*(7–9), 869–896, doi:10.1016/j.quascirev.2004.07.015.

Giannakopoulos, C., M. P. Chipperfield, K. S. Law, and J. A. Pyle (1999), Validation and intercomparison of wet and dry deposition schemes using 210Pb in a global three-dimensional offline chemical transport model, *J. Geophys. Res.*, *104*, 23,761–23,784, doi:10.1029/1999JD900392.

Giannakopoulos, C., P. Good, K. S. Law, K.-Y. Wang, E. Akylas, and A. Koussis (2004), Rainfall parameterization in an off-line chemical transport model, *Atmos. Sci. Lett.*, *5*, doi:10.1002/asl.68.

Gong, S. L., L. A. Barrie, J. M. Prospero, D. L. Savoie, G. P. Ayers, J.-P. Blanchet, and L. Spacek (1997), Modeling sea-salt aerosols in the atmosphere: 2. Atmospheric concentrations and fluxes, *J. Geophys. Res.*, *102*(D3), 3819–3830.

Gong, S. L., L. A. Barrie, and M. Lazare (2002), Canadian Aerosol Module (CAM): A size-segregated simulation of atmospheric aerosol processes for climate and air quality models 2. Global sea-salt aerosol and its budgets, *J. Geophys. Res.*, *107*(D24), 4779, doi:10.1029/2001JD002004.

Holland, P. R., and R. Kwok (2012), Wind-driven trends in Antarctic sea-ice drift, *Nat. Geosci.*, *5*, doi:10.1038/NGEO1627.

Holtslag, A. A. M., and B. A. Boville (1993), Local versus nonlocal boundary-layer diffusion in a global climate model, *J. Clim.*, *6*, 1825–1842, doi:10.1175/1520-0442(1993)006<1825:LVNBLD>2.0.CO;2.

Iizuka, Y., B. Delmonte, I. Oyabu, T. Karlin, V. Maggi, S. Albani, M. Fukui, T. Hondoh, and M. Hansson (2013), Sulphate and chloride aerosols during Holocene and last glacial periods preserved in the Talos Dome Ice Core, a peripheral region of Antarctica, *Tellus Ser. B Chem. Phys. Meteorol.*, *65*, doi:10.3402/tellusb.v65i0.20197.

Jaeger, L. (1976), Monatskarten des Niederschlags fur die ganze Erde, *Berichte des Deutschen Wetterdienstes*, *18*, 1–38.

Jones, A. E., P. S. Anderson, E. W. Wolff, J. Turner, A. M. Rankin, and S. R. Colwell (2006), A role for newly forming sea ice in springtime polar tropospheric ozone loss? Observational evidence from Halley station, Antarctica, *J. Geophys. Res.*, *111*, D08306, doi:10.1029/2005JD006566.

Jones, A. E., P. S. Anderson, M. Begoin, N. Brough, M. A. Hutterli, G. J. Marshall, A. Richter, H. K. Roscoe, and E. W. Wolff (2009), BrO, blizzards, and drivers of polar tropospheric ozone depletion events, *Atmos. Chem. Phys.*, *9*(14), doi:10.5194/acp-9-4639-2009.

Jones, A. E., P. S. Anderson, E. W. Wolff, H. K. Roscoe, G. J. Marshall, A. Richter, N. Brough, and S. R. Colwell (2010), Vertical structure of Antarctic tropospheric ozone depletion events: Characteristics and broader implications, *Atmos. Chem. Phys.*, *10*(16), doi:10.5194/acp-10-7775-2010.

Jourdain, B., S. Preunkert, O. Cerri, H. Castebrunet, R. Udisti, and M. Legrand (2008), Year-round record of size-segregated aerosol composition in central Antarctica (Concordia station): Implications for the degree of fractionation of sea-salt particles, *J. Geophys. Res.*, *113*, D14308, doi:10.1029/2007JD009584.

Jouzel, J., et al. (2007), Orbital and millennial Antarctic climate variability over the past 800,000 years, *Science*, *317*, 793–796, doi:10.1126/science.1141038.

Kaleschke, L., et al. (2004), Frost flowers on sea ice as a source of sea salt and their influence on tropospheric halogen chemistry, *Geophys. Res. Lett.*, *31*, L16114, doi:10.1029/2004GL020655.

Kaspari, S., D. A. Dixon, S. B. Sneed, and M. J. Handley (2005), Sources and transport pathways of marine aerosol species into West Antarctica, *Ann. Glaciol.*, *41*(1), 1–9, doi:10.3189/172756405781813221.

Kurtz, N. T., T. Markus, S. L. Farrell, D. L. Worthen, and L. N. Boisvert (2011), Observations of recent Arctic sea ice volume loss and its impact on ocean-atmosphere energy exchange and ice production, *J. Geophys. Res.*, *116*, C04015, doi:10.1029/2010JC006235.

Legates, D. R., and C. J. Willmott (1990), Mean seasonal and spatial variability in gauge-corrected, global precipitation, *Int. J. Climatol.*, *10*, 111–127.

Levine, J. G., P. Braesicke, N. R. P. Harris, N. H. Savage, and J. A. Pyle (2007), Pathways and timescales for troposphere-to-stratosphere transport via the tropical tropopause layer and their relevance for very short lived substances, *J. Geophys. Res.*, *112*, D04308, doi:10.1029/2005JD006940.

Levine, J. G., E. W. Wolff, A. E. Jones, M. A. Hutterli, O. Wild, G. D. Carver, and J. A. Pyle (2011a), In search of an ice core signal to differentiate between source-driven and sink-driven changes in atmospheric methane, *J. Geophys. Res.*, *116*, D05305, doi:10.1029/2010JD014878.

Levine, J. G., E. W. Wolff, A. E. Jones, L. C. Sime, P. J. Valdes, A. T. Archibald, G. D. Carver, N. J. Warwick, and J. A. Pyle (2011b), Reconciling the changes in atmospheric methane sources and sinks between the Last Glacial Maximum and the pre-industrial era, *Geophys. Res. Lett.*, *38*, L23804, doi:10.1029/2011GL049545.

Levine, J. G., E. W. Wolff, P. O. Hopcroft, and P. J. Valdes (2012), Controls on the tropospheric oxidizing capacity during an idealized Dansgaard-Oeschger event, and their implications for the rapid rises in atmospheric methane during the last glacial period, *Geophys. Res. Lett.*, *39*, L12805, doi:10.1029/2012GL051866.

Loulergue, L., A. Schilt, R. Spahni, V. Masson-Delmotte, T. Blunier, B. Lemieux, J.-M. Barnola, D. Raynaud, T. F. Stocker, and J. Chappellaz (2008), Orbital and millennial-scale features of atmospheric CH_4 over the past 800,000 years, *Nature*, *453*, 383–386, doi:10.1038/nature06950.

Lüthi, D., et al. (2008), High-resolution carbon dioxide concentration record 650,000–800,000 years before present, *Nature*, *453*, 379–382, doi:10.1038/nature06949.

Mahowald, N. M., J. F. Lamarque, X. X. Tie, and E. Wolff (2006), Sea-salt aerosol response to climate change: Last Glacial Maximum, preindustrial, and doubled carbon dioxide climates, *J. Geophys. Res.*, *111*, D05303, doi:10.1029/2005JD006459.

Monahan, E. C., et al. (1986), A model of marine aerosol generation via whitecaps and wave disruption, in *Oceanic Whitecaps and Their Role in Air-Sea Exchange Processes*, edited by E. C. Monahan and G. MacNiocaill, pp. 167–174, Springer, New York.

Massom, R. A., et al. (2001), Snow on Antarctic sea ice, *Rev. Geophys.*, *39*(3), 413–445, doi:10.1029/2000RG000085.

Parmentier, F.-J. W., T. R. Christensen, L. L. Sorensen, S. Rysgaard, A. D. McGuire, P. A. Miller, and D. A. Walker (2013), The impact of lower sea-ice extent on Arctic greenhouse-gas exchange, *Nat. Clim. Change*, *3*(3), doi:10.1038/NCLIMATE1784.

Paul, A., and C. Schäfer-Neth (2003a), Global LGM SST and salinity reconstruction, IGBP PAGES/World Data Centre for Paleoclimatology, Boulder Data Contribution Series 2003-046, NOAA/NGDC Paleoclimatology Program, Boulder, Colo.

Paul, A., and C. Schäfer-Neth (2003b), Modeling the water masses of the Atlantic Ocean at the Last Glacial Maximum, *Paleoceanography*, *18*(3), 1058, doi:10.1029/2002PA000783.

Perovich, D. K., and J. A. Richter-Menge (1994), Surface characteristics of lead ice, *J. Geophys. Res.*, *99*(C8), 16,341–16,350, doi:10.1029/94JC01194.

Petit, J. R., and B. Delmonte (2009), A model for large glacial-interglacial climate-induced changes in dust and sea salt concentrations in deep ice cores (central Antarctica): Paleoclimatic implications and prospects for refining ice core chronologies, *Tellus*, *61B*, 768–790.

Petit, J. R., et al. (1999), Climate and atmospheric history of the past 420,000 years from the Vostok ice core, Antarctica, *Nature*, *399*, doi:10.1038/20859.

Pflaumann, U., et al. (2003), Glacial North Atlantic: Sea-surface conditions reconstructed by GLAMAP 2000, *Paleoceanography*, *18*(3), 1065, doi:10.1029/2002PA000774.

Prather, M. J. (1986), Numerical advection by conservation of second-order moments, *J. Geophys. Res.*, *91*, 6671–6681, doi:10.1029/JD091iD06p06671.

Rankin, A. M., and E. W. Wolff (2003), A year-long record of size-segregated aerosol composition at Halley, Antarctica, *J. Geophys. Res.*, *108*(D24), 4775, doi:10.1029/2003JD003993.

Rankin, A. M., V. Auld, and E. W. Wolff (2000), Frost flowers as a source of fractionated sea salt aerosol in the polar regions, *Geophys. Res. Lett.*, *27*(21), 3469–3472, doi:10.1029/2000GL011771.

Rankin, A. M., E. W. Wolff, and S. Martin (2002), Frost flowers: Implications for tropospheric chemistry and ice core interpretation, *J. Geophys. Res.*, *107*(D23), 4683, doi:10.1029/2002JD002492.

Rankin, A. M., E. W. Wolff, and R. Mulvaney (2004), A reinterpretation of sea-salt records in Greenland and Antarctic ice cores?, *Ann. Glaciol.*, *39*, 276–282, doi:10.3189/172756404781814681.

Rayner, N. A., D. E. Parker, E. B. Horton, C. K. Folland, L. V. Alexander, D. P. Rowell, E. C. Kent, and A. Kaplan (2003), Global analyses of sea surface temperature, sea ice, and night marine air temperature since the late nineteenth century, *J. Geophys. Res.*, *108*(D14), 4407, doi:10.1029/2002JD002670.

Reader, M. C., and N. McFarlane (2003), Sea-salt aerosol distribution during the Last Glacial Maximum and its implications for mineral dust, *J. Geophys. Res.*, *108*(D8), 4253, doi:10.1029/2002JD002063.

Roscoe, H. K., B. Brooks, A. V. Jackson, M. H. Smith, S. J. Walker, R. W. Obbard, and E. W. Wolff (2011), Frost flowers in the laboratory: Growth, characteristics, aerosol, and the underlying sea ice, *J. Geophys. Res.*, *116*, D12301, doi:10.1029/2010JD015144.

Röthlisberger, R., et al. (2008), The Southern Hemisphere at glacial terminations: Insights from the Dome C ice core, *Clim. Past*, *4*, 345–356.

Röthlisberger, R., X. Crosta, N. J. Abram, L. Armand, and E. W. Wolff (2010), Potential and limitations of marine and ice core sea ice proxies: An example from the Indian Ocean sector, *Quat. Sci. Rev.*, *29*(1–2), 296–302.

Saiz-Lopez, A., A. S. Mahajan, R. A. Salmon, S. J. Bauguitte, A. E. Jones, H. K. Roscoe, and J. M. C. Plane (2007), Boundary layer halogens in coastal Antarctica, *Science*, *317*(5836), doi:10.1126/science.1141408.

Sarnthein, M., et al. (2003), Overview of Glacial Atlantic Ocean Mapping (GLAMAP 2000), *Paleoceanography*, *18*(2), 1030, doi:10.1029/2002PA000769.

Schmidt, R. A. (1982), Vertical profiles of wind speed, snow concentration, and humidity in blowing snow, *Boundary Layer Meteorol.*, *23*, 223–246.

Schüpbach, S., U. Federer, S. Albani, C. Barbante, T. F. Stocker, and H. Fischer (2013), Sources and transport of dust to East Antarctica: New insights from high-resolution terrestrial and marine aerosol records from the Talos Dome ice core, *Clim. Past Discuss.*, *9*, 3321–3370, doi:10.5194/cpd-9-3321-2013.

SethuRaman, S., and G. S. Raynor (1975), Surface drag coefficient dependence on the aerodynamic roughness of the sea, *J. Geophys. Res.*, *80*(36), 4983–4988, doi:10.1029/JC080i036p04983.

Steig, E. J., D. L. Morse, E. D. Waddington, M. Stuiver, P. M. Grootes, P. A. Mayewski, M. S. Twickler, and S. I. Whitlow (2000), Wisconsinan and Holocene climate history from an ice core at Taylor Dome, western Ross Embayment, Antarctica, *Geografiska Annaler Ser. A Phys. Geography*, *82A*(2–3), doi:10.1111/j.0435-3676.2000.00122.x.

Stephens, B. B., and R. F. Keeling (2000), The influence of Antarctic sea ice on glacial-interglacial CO2 variations, *Nature*, *404*, 171–174.

Tiedtke, M. (1989), A comprehensive mass flux scheme for cumulus parameterization in large-scale models, *Mon. Weather Rev.*, *117*, 1779–1800, doi:10.1175/1520-0493(1989)117<1779:ACMFSF>2.0.CO;2.

Udisti, R., et al. (2012), Sea spray aerosol in central Antarctica. Present atmospheric behaviour and implications for paleoclimatic reconstructions, *Atmos. Environ.*, *52*, 109–120.

Wagenbach, D., F. Ducroz, R. Mulvaney, L. Keck, A. Minikin, M. Legrand, J. S. Hall, and E. W. Wolff (1998), Seasalt aerosol in coastal Antarctic regions, *J. Geophys. Res.*, *103*, 10,961–10,974, doi:10.1029/97JD01804.

Warwick, N. J., J. A. Pyle, and D. E. Shallcross (2006), Global modelling of the atmospheric methyl bromide budget, *J. Atmos. Chem.*, *54*(2), 133–159, doi:10.1007/s10874-006-9020-3.

Warwick, N. J., et al. (2013), A global model study of the impact of land-use change in Borneo on atmospheric composition, *Atmos. Chem. Phys.*, *13*, 9183–9194, doi:10.5194/acp-13-9183-2013.

Weller, R., and D. Wagenbach (2007), Year-round chemical aerosol records in continental Antarctica obtained by automatic samplings, *Tellus*, *59*, 755–765.

Wolff, E. W., A. M. Rankin, and R. Röthlisberger (2003), An ice core indicator of Antarctic sea ice production?, *Geophys. Res. Lett.*, *30*(22), 2158, doi:10.1029/2003GL018454.

Wolff, E. W., et al. (2006), Southern-Ocean sea-ice extent, productivity and iron flux over the past eight glacial cycles, *Nature*, *440*, 491–496, doi:10.1038/nature04614.

Wolff, E. W., et al. (2010), Changes in environment over the last 800,000 years from chemical analysis of the EPICA Dome C ice core, *Quat. Sci. Rev.*, *29*, 285–295.

Worby, A. P., C. A. Geiger, M. J. Paget, M. L. Van Woert, S. F. Ackley, and T. L. DeLiberty (2008), Thickness distribution of Antarctic sea ice, *J. Geophys. Res.*, *113*, C05S92, doi:10.1029/2007JC004254.

Sato, H., T. Suzuki, M. Hirabayashi, Y. Iizuka, H. Motoyama, and Y. Fujii (2013), Mineral and sea-salt aerosol fluxes over the last 340 kyr reconstructed from the total concentration of Al and Na in the Dome Fuji ice core, *Atmos. Clim. Sci.*, *3*(2), doi:10.4236/acs.2013.32020.

Yang, X., R. A. Cox, N. J. Warwick, J. A. Pyle, G. D. Carver, F. M. O'Connor, and N. H. Savage (2005), Tropospheric bromine chemistry and its impacts on ozone: A model study, *J. Geophys. Res.*, *110*, D23311, doi:10.1029/2005JD006244.

Yang, X., J. A. Pyle, and R. A. Cox (2008), Sea salt aerosol production and bromine release: Role of snow on sea ice, *Geophys. Res. Lett.*, *35*, L16815, doi:10.1029/2008GL034536.

Yang, X., J. A. Pyle, R. A. Cox, N. Theys, and M. Van Roozendael (2010), Snow-sourced bromine and its implications for polar tropospheric ozone, *Atmos. Chem. Phys.*, *10*, 7763–7773, doi:10.5194/acp-10-7763-2010.